The University of Alberta
Printing Department
Edmonton, Alberta

THE UNIVERSITY OF ALBERTA

INVESTIGATION OF THE SPINS OF THE LOW LYING LEVELS OF ^{64}Cu VIA THE ^{64}Ni(p,nγ)^{64}Cu REACTION

by

© Mark Mondelet Drum

A THESIS

SUBMITTED TO THE FACULTY OF GRADUATE STUDIES

IN PARTIAL FULFILLMENT OF THE REQUIREMENTS FOR THE DEGREE

OF MASTER OF SCIENCE

DEPARTMENT OF PHYSICS

EDMONTON, ALBERTA

Spring 1970

UNIVERSITY OF ALBERTA

FACULTY OF GRADUATE STUDIES

The undersigned certify that they have read, and recommend to the Faculty of Graduate Studies for acceptance, a thesis entitled INVESTIGATION OF THE SPINS OF THE LOW LYING LEVELS OF ^{64}Cu VIA THE ^{64}Ni(p,nγ)^{64}Cu REACTION submitted by Mark Mondelet Drum in partial fulfillment of the requirements for the degree of Master of Science.

ABSTRACT

A study of the gamma radiation following the $^{64}Ni(p,n\gamma)^{64}Cu$ reaction has yielded decay branching ratios, spin assignments, and multipole mixing ratios for the levels in ^{64}Cu below 700 keV excitation. Gamma-ray angular distributions were measured for incident proton energies within 200 keV of threshold for the levels of interest in ^{64}Cu. Spins and mixing ratios were obtained from comparison of the experimental distributions with the predictions of the compound nuclear statistical model. Spin assignments have been obtained for the 159 keV (2^+), 278 keV (2^+), 344 keV ($1^+,2^+$), 362 keV (3^+), 608 keV (2^+) and 663 keV ($0^+,1^+,2^+$) levels in ^{64}Cu. Parities were deduced from the $^{63}Cu(d,p)^{64}Cu$ reaction (Pa 69). Mixing ratios of ground state transitions have been determined using the Rose-Brink convention for the 159 keV ($\delta = -0.07 \pm 0.02$ or $-2.39\ ^{+0.15}_{-0.24}$), 278 keV ($\delta = -0.16 \pm 0.02$ or $-1.69\ ^{+0.14}_{-0.23}$), and 608 keV ($\delta = -0.07 \pm 0.01$ or $-2.14\ ^{+0.18}_{-0.26}$) gamma rays; for the 362 keV to 159 keV transition $\delta = -0.08 \pm 0.02$.

An attempt has been made to account for the spins of these low lying levels from considerations of simple shell model particle configurations.

The dependence of the predicted a_K coefficients of the compound statistical nuclear model as a function of the transmission coefficients has been discussed in the appendix.

ACKNOWLEDGEMENTS

I would like to thank my supervisor, Dr. D.M. Sheppard for his encouragement and patient assistance throughout all phases of the experiment.

I am especially grateful to Peter Green and Dr. Barry Robertson for their assistance in data collection and the innumerable helpful discussions on all aspects of the work.

I am indepted to Georges Carola and Dr. William Olsen for their numerous explanations of the electronics and to my other colleagues, Paul Gutowski, Woon Chung and Ed Wong, for their unselfish assistance during the running of the experiment.

The cooperation of technical staff, in particular slim Jock Elliott, Lars Holm, Paul Karvonen, Ron Popik and Harold Fodchuk has been deeply appreciated.

I would also like to thank Dr. Kenneth Dawson for his helpful bits of useful information regarding the SDS 920 computer. (May the Honeywell one day wear the "Dawsonized" seal of approval.)

To Miss Audrey Forman I offer my sympathy and thanks for the typing of this manuscript.

Finally, I wish to acknowledge the financial assistance of the National Research Council and the Department of Physics.

TABLE OF CONTENTS

LIST OF TABLES

LIST OF FIGURES

APPENDIX

CHAPTER 1

INTRODUCTION

1.1 Theoretical Motivation

The isotopes within the 1f - 2p shell have only recently become of interest to nuclear physicists. Investigations, both experimentally and theoretically, of nuclei with neutron number N = 29, 31 and 33 have provided useful information regarding the validity of various models (e.g. the shell and core-particle models) in 1f - 2p shell, however little work has been carried out for N = 35 nuclei. In particular the odd-odd nuclei ^{64}Cu has received little consideration. With respect to the shell model interpretation of the low lying states of this nuclei, regional systematics suggests the dominance of configurations based on the coupling of a $2p^{3/2}$ proton to $2p^{3/2}$, $1f^{5/2}$, and $2p^{1/2}$ neutron orbitals. It would be expected that the lowest seniority coupling of these orbitals would give use to the low-lying level structure of ^{64}Cu. Although the level scheme for ^{64}Cu has been determined the spin assignments for these states are still unknown. It was felt that a detailed study of the gamma-ray decay of the low-lying levels of ^{64}Cu would provide this information which in turn would be of extreme aid in determining their detailed character.

1.2 Previous Experimental Work on ^{64}Cu

During the last few years the low-lying states of ^{64}Cu have been the subject of several experimental investigations. Unfortunately many details of the level structure remain either unknown or uncertain.

An early (d,p) stripping investigation of de Figueiredo et al. (Fi 58) established excitation energies up to about 3.8 MeV but did not include the charged particle angular distributions and therefore specification of the angular momenta and parity of states in ^{64}Cu was lacking. Other stripping reaction studies of the levels of ^{64}Cu (Hj 66,Yo 68) with poor experimental energy resolution and low cross sections prevented the extraction of reliable ℓ values. However more recently Park and Daehnick (Pa 69) have been able to present ℓ_n assignments and J^π limits for levels in ^{64}Cu up to 3 MeV excitation based on DWBA analysis of some high resolution $Zn^{66}(d,\alpha)^{64}Cu$ and $^{63}Cu(d,p)^{64}Cu$ reaction studies. (table 1)

Investigations of the gamma rays decaying from thermal neutron capture states following the $^{63}Cu(n,\gamma)^{64}Cu$ reaction (Ba 53,Ve 61,Ba 64, Ko 65,Tr 57,Co 67) have revealed some interesting and useful features of the level structure of ^{64}Cu but, for the most part, have not possessed the necessary detail required to specify the properties of many of these states. In particular, these studies have yielded spin assignments for a number of excited states which have been either uncertain or conflicting with other results. Recently, however, a thermal neutron-capture γ-ray study by Shera and Bolotin (Sh 68) produced spin assignments based on intensity arguments for several of the low-lying states of ^{64}Cu. One

of the prime considerations of their arguments was the assumption that quadrupole radiation should not be particularly enhanced in this mass region and that when possible, dipole radiation would be the dominate mode of decay. Specifically, it was considered that the γ-ray cascade of the 0.574 MeV level via the 0.362 MeV and 0.278 MeV levels to the ground state represented a series of M1 transitions. As a result the 0.574, 0.362, and 0.278 levels were assigned J^{π} values of 4^+, 3^+, and 2^+ respectively (table 1). Although these spin assignments were later shown to be consistant with the qualitative results of Park and Daehnick (Pa 69) they should only be considered as tentative.

The γ-rays decaying from thermal neutron-capture states have also been the subject of several circular polarization measurements. The results of these measurements have led to a multitude of conflicting spin assignments. The most recent Kopecky et al. (Ko 69) (table 1), reports spin assignments of 1^+ and 3^+ for the 0.278 MeV and 0.608 MeV levels respectively. These results disgree with all previous assignments.

The thermal neutron capture γ-ray reaction was also studied by du Toit and Bollinger (To 61) in order to obtain an upper limit of 0.3 ns for the half-life of the 0.159 MeV and 0.278 MeV excited states of ^{64}Cu.

Recently the ^{64}Ni(p,nγ)^{64}Cu (Du 68,We 69) reaction has been investigated in an attempt to determine some of the spins of the low lying excited states of ^{64}Cu. Although angular correlation measurements by Wellborne and Buccino (We 69) indicate J^{π} values of 2^+ and 3^+ for the 0.278 MeV and 0.362 MeV excited states respectively, in general the

spin assignments for the low-lying levels of ^{64}Cu are unknown or uncertain.

Shortly before completion of the present work Davidson et al. (Da 70) presented spin assignments for the low-lying states of ^{64}Cu determined via a ^{64}Ni(p,nγ)^{64}Cu reaction. These results are listed in table 1 together with the assignments determined from the present study.

TABLE 1

A Summary of the Results of Previous Investigations on the Low Lying States of ^{64}Cu

	(Pa 69)				(Sh 68)		(Ko 69)	(Da 70)	Present
	$^{63}Cu(d,p)$		$^{66}Zn(d,\alpha)$		$^{63}Cu(n,\gamma)^{\dagger}$		$^{63}Cu(n,\gamma)^{\dagger\dagger}$	$^{64}Ni(p,n\gamma)$	Work
E^*	ℓ_n	J^π	L	J^π	E^*	J^π	J^π	J^π	J^π
0	$\{^1_3$	$1^+ - 3^+$	$\{^0_2$	1^+	0	1^+	1^+	1^+	1^+
0.158	$\{^1_3$	$1^+ - 3^+$	$\{^2_0$	$2^+(1^+)$	0.159	(2^+)		2^+	2^+
0.278	$\{^1_3$	$1^+ - 3^+$	2	$2^+(1^+,3^+)$	0.278	2^+	1^+	2^+	2^+
0.342	1	$0^+ - 3^+$		$(2^+,0^+)$	0.344	$(1^+,2^+)$		$(1^+,2^+)$	$(1^+,2^+)$
0.361	$\{^1_3$	$1^+ - 3^+$	4	3^+	0.362	(3^+)		(3^+)	3^+
0.573	3	$1^+ - 4^+$	4	$4^+(3^+)$	0.574	(4^+)	$(1 ,2^+)$		
0.606	1	$0^+ - 3^+$	2	$2^+(1^+,3^+)$	0.609	$(1^+,2^+)$	1^+	2^+	2^+
0.667	1	$0^+ - 3^+$	4	3^+	0.663	$(1^+,2^+)$		$(1^+,2^+)$	$(0^+,1^+,2^+)$

E^* is in MeV.

† Thermal Capture

†† Circular Polarization

CHAPTER 2

THEORETICAL INTERPRETATION

2.1 Physical Interpretation of the A(a,bγ)B Reaction

The measurement of the gamma-ray angular distributions following the decay of an aligned nuclear state is frequently used to determine the spin of the nuclear level. Consider the reaction A(a,b)B which leads to an excited state in B (total angular momentum J_B) which then de-excites by γ-ray emission to a lower-lying state in B (total angular momentum J_C).

The angular distribution of a gamma ray transition from a state of spin J_B to a state of spin J_C is given by

$$W(\theta) = \sum_{\ell\ m\ m'} P(m) \left| \langle J_B m | J_C m' \ell m-m' \rangle \right|^2 F_\ell^{m-m'}(\theta)$$

(Li 64); P(m) is the population parameter (probability that the m^{th} state is populated) for the m^{th} magnetic substate of J_B (there are $2J_B+1$ possible magnetic substates or possible orientations with respect to an axis of quantization), $\langle J_B m | J_C m' \ell m-m' \rangle$ is a Clebsch-Gordan coefficient and $F_\ell^{m-m'}(\theta)$ is the radiation pattern for multipolarity ℓ and magnetic quantum number change m-m'.

The population parameters P(m) of the decaying state together with the multipolarity ℓ determine the nature of the angular distribution; the amount of anisotropy being dependant primarily on P(m). If the magnetic

substates of the initial state are equally populated there is no preferred spatial direction and all orientations of the total angular momentum are equally probable; the gamma-ray will be emitted in all directions with equal probability (an isotropic angular distribution). Under such conditions little information concerning the spin of the decaying state or the nature of the decay radiation can be obtained. In order to obtain useful information aligned or polarized nuclear states are required. An aligned nuclear state has positive and negative magnetic substates equally populated, i.e. $P(m)=P(-m)$, (if $P(m) \neq P(-m)$ the state is said to be polarized).

Consider the reaction in the incident channel. The incoming projectile a (spin s_a) may be decomposed into contributions of given orbital angular momentum ℓ_a or given total angular momentum j_a ($= |\vec{\ell}_a + \vec{s}_a|$). The incident total angular momenta j_a and the total angular momentum J_A of the target can couple vectorially to form a state in the intermediate nucleus J_{int} ($= |\vec{j}_a + \vec{J}_A| = (|\vec{\ell}_a + \vec{s}_a + \vec{J}_A|)$. If we consider the reaction to take place in states of channel spin S ($=|\vec{s}_a + \vec{J}_A|$) which can couple with the orbital angular momentum of the partial waves ℓ_a to give J_{int} ($|\vec{\ell}_a + \vec{S}|$) then the states J_{int} will have definite parity given by the product of $(-1)^{\ell a}$ and the intrinsic parities of the target and the projectile. Since the orbital angular momentum of the incoming projectile, ℓ_a, is in the plane perpendicular to the beam direction (the axis of quantization) $m_{\ell_a} = 0$ and only the possible orientations of the target spin J_A and the intrinsic spin of the projectile s_a will contribute to the population of the magnetic substates of the intermediate nucleus. In general the intermediate states will be

aligned, the amount of alignment being dependent on the target spin and the spin of the captured nucleon. The aligned intermediate state may now decay by particle or γ-ray emission. If it is energetically possible neutron emission will usually occur. The neutron which has total momentum $j_b = |\vec{\ell}_b + \vec{s}_b|$ will tend to de-align the intermediate state since the neutron can be emitted in any direction. The projection of ℓ_b on the quantization axis is not necessarily zero and additional magnetic substates in the residual nuclear state can be populated. The final state will in general be less strongly aligned that the intermediate state. If however the reaction takes place near the threshold for neutron emission, the emitted neutron will be of low energy and $\ell_b = 0$ partial waves will predominate. Consequently $m_{\ell_b} = 0$ and only the possible spin orientations of the neutron m_{s_b} will contribute to the de-alignment of the intermediate state. Although higher-order outgoing partial waves ($\ell_b \geq 1$) are present the amount of admixture with the predominant s-wave is small and results only in a small reduction in the alignment of the residual state. Consequently for the (p,n) reaction the magnetic substates of the residual states will only have appreciable populations up to $|m| = J_A + 1$. As long as $J_B > J_A + 1$, the residual state will be aligned and anisotropic gamma ray angular distributions are to be expected. Since the anisotropy of the gamma ray decay from a state of spin J_B is dependent on the spin of the final state J_c, this spin must be known in order to make a unique determination of the spin J_B.

2.2 Assumptions of the Statistical Model

The analysis of the (p,nγ) reaction can be carried out using the compound nuclear statistical model of Sheldon and van Patter (Sh 66). The model basically contains the compound nuclear theory of Hauser and Feshbach (Ha 52) together with the assumptions of the random phase approximation and intermediate states of definite parity. The basic premise of the statistical approach is that the reaction proceeds via a large number of intermediate levels and the fluctuations in the reaction cross section, due to the interference between overlapping levels in the compound nucleus will average out to be zero.

Physical justification for this assumption is given in the following argument. For proton-induced reactions on medium weight nuclei the Q-value for the formation of the intermediate nucleus is typically of the order of 8 MeV. This excitation energy, in the intermediate nucleus is sufficient to excite states with many particle configurations and the level density in the compound nucleus is expected to be high (~1 level per keV). For targets which are thick enough to ensure that a large number of intermediate states are excited the interference terms for the overlapping levels in the compound nucleus will average to zero, (Er 63).

Interference between the various partial waves for both the incoming and outgoing waves should also be considered. Vogt (Vo 68) however, points out that since the matrix elements are random there is no coherent contribution to the amplitude for a given partial wave due to interference with other partial waves in both the incoming and outgoing channels. A

similar argument for the non-interference effect of the partial waves in the outgoing channel has been given by Blatt & Weisskopf (Bl 52). Since the particles decaying from the compound nucleus are often unobserved, the interference effects between the various partial waves must be averaged over all space with the result that the interference terms vanish.

The random phase of the matrix elements together with the fact that the cross-section is energy-averaged enables the absolute square of the matrix elements to be expressed in terms of energy-averaged transmission coefficients.

2.3 The Transmission Coefficients

The matrix elements for the reaction and hence the corresponding reaction cross-section are defined by amplitudes in the various reaction channels. To determine these amplitudes all the possible two-body interactions between the nucleons of the nucleus and the projectile should be considered. However, except for the simplest of cases, this approach is much too complicated. Consequently a phenomenological model of the interaction is adopted. The approximation that the many-body problem can be reduced to two structureless bodies interacting through an average potential is known as the optical model.

The nuclear optical potential which influences an incident nucleon has the form

$$V_N(r) = \frac{-V_0 - C_0E}{1 + e^{(r-R_r)/a_r}} - i(W_0 + C_1E)e^{-(R_i-r)^2/a_i} + V_{SO}$$

where E is the relative kinetic energy of the target-projectile pair, V_0 is the real well depth, W_0 is the imaginary well depth, R_r and R_i are the radius parameters for the real and imaginary well respectively, a_r and a_i are the corresponding well diffuseness parameters, and V_{SO} is the spin-orbit potential. The nuclear potential contains real and imaginary terms that account for both refraction and absorption of the incident particle flux. Transmission coefficients can be defined in terms of the absorption of each partial wave; (these can be obtained by analyzing the elastic scattering data for the target-projectile pair). The scattering and absorption cross sections can each be expressed in terms of complex phase shifts in the optical model.

The relation between the wave amplitudes and the transmission coefficients can be seen in the following manner. When all the nucleons of the system are close together a compound nucleus is said to exist; when any two groups of nucleons are separated from each other a reaction channel or elastic (incident) channel is said to exist. The matrix elements linking the initial and final states through the nuclear potential and hence the reaction cross section can be expressed in terms of the wave amplitudes in the incident and reaction channels. More precisely the amplitudes of the various partial waves in the reaction channel will be related to the partial wave amplitudes in the incident channel through the collision or reaction matrix.

For each reaction channel the wave function describing the reaction pair can be expressed in the channel-spin representation as

$$\Psi_\alpha = \phi_\alpha \psi_\alpha \ .$$

ψ_α contains the angular dependence of the wave function

$$\psi_\alpha = r_\alpha^{-1} \Phi_\alpha \sum_{m_\ell} \sum_{m_s} (\ell S m_\ell m_S | J m_J) i^\ell Y_\ell^{m_\ell} \chi_S^{m_S}$$

where r_α is the relative separation of the pair in the reaction channel, Φ_α describes the intrinsic spatial wave functions of the two particles in the reaction channel, $i^\ell Y_\ell^{m_\ell}$ is a spherical harmonic describing their relative orbital angular momentum ℓ (z-component m_ℓ), $\chi_S^{m_S}$ is the wave function of the coupled intrinsic spins (channel spin) of the two particles, $(\ell S m_\ell m_S | J m_J)$ is a Clebsch-Gordan coefficient, and J is the total angular momentum of the system (magnetic projection m_J). The radial wave function ϕ_α is expressed in terms of the regular and irregular solutions (coulomb wave functions) of the equation

$$\frac{d^2\phi_\alpha}{dr_\alpha^2} - \frac{\ell(\ell+1)}{r_\alpha^2} \phi_\alpha - \frac{2\eta_\alpha k_\alpha \phi_\alpha}{r_\alpha} + k^2 \phi_\alpha = 0 \ .$$

ϕ_α is a linear combination of $F_\ell(\eta,kr)$ and $G_\ell(\eta,kr)$, where for large kr

$$F_\ell(\eta,kr) \rightarrow \sin(kr - \eta \ln 2kr - \tfrac{1}{2}\ell\pi + \delta_\ell)$$

and

$$G_\ell(\eta,kr) \rightarrow \cos(kr - \eta \ln 2kr - \tfrac{1}{2}\ell\pi + \delta_\ell) \ .$$

The quantity $\eta (\equiv z_1 z_2 e^2/h\upsilon)$ is the coulomb parameter, $\sigma_\ell (\equiv \arctan \Gamma(\ell + 1 + i\eta))$ is the coulomb phase shift and υ is the relative velocity of

the pair.

For uncharged particles the coulomb functions F_ℓ and G_ℓ are the spherical Bessel and Neumann functions respectively.

The radial wave function can be expressed as a combination of incoming and outgoing waves, namely as

$$\phi_\alpha \simeq [A^\alpha_{\ell SJ}(G_\ell(\eta,kr) - iF_\ell(\eta,kr)) + B^\alpha_{\ell SJ}(G_\ell(\eta,kr) + iF_\ell(\eta,kr))$$

where $A^\alpha_{\ell SJ}$ and $B^\alpha_{\ell SJ}$ are the amplitude coefficients for the incoming and outgoing partial waves. The ratio of $B^\alpha_{\ell SJ}$ to $A^\alpha_{\ell SJ}$ is the complex scattering amplitude and can be expressed by the elements of the collision matrix. That is

$$B^\alpha_{\ell SJ} = \sum_{\ell'S'} U^J_{\alpha\ell S,\alpha\ell'S'} A^\alpha_{\ell'S'J}$$

more precisely the ratio of these amplitudes can be expressed directly in terms of the complex optical model phase shift as

$$\frac{B_{\ell SJ}}{A_{\ell SJ}} = \eta_{\ell SJ} = \exp(2i\delta_{\ell SJ})$$

The transmission coefficients $T_{\ell sj}$ in the optical model are usually calculated in the j-j representation which in terms of the complex phase shift $\delta_{\ell sj}$ gives

$$T_{\ell sj} = 1 - |\exp(2i\delta_{\ell sj})|^2$$

The transmission coefficients in the (jj)-representation are related to the transmission coefficients in the (ℓS)-representation by

$$T_{\ell SJ} = \sum_{s} (2j + 1)\ (2s + 1)\ W^2(\ell IJS;js) T_{\ell sj}$$

where I is the intrinsic spin of the "target" nucleus. The transmission coefficients in the incident channel represent the probability that a partial wave of order ℓ will be absorbed by the target nucleus to result in the formation of a coupound nucleus. The transmission coefficients in the reaction channel can be obtained by considering the inverse reaction and the use of reciprocity (detailed balance).

The reaction channel and its reverse are closely related by the concept of time reversal and reciprocity. In fact, except for statistical factors the cross sections for the reactions A(a,b)B and B(b,a)A are the same.

$$k_a^2(2S_a+1)\ (2S_A+1)\ \frac{d\sigma}{d\Omega}\ (a,b) = k_b^2\ (2S_b+1)\ (2S_B+1)\ \frac{d\sigma}{d\Omega}\ (b,a)$$

Thus in order to calculate the probability that a compound nucleus, say ^{65}Cu, will emit a neutron and leave the residual nucleus in one of its excited states the reverse problem where neutrons are considered to be incident on the particular excited state of ^{64}Cu may be treated. Once the inverse reaction has been solved the original problem of the decay of the compound nucleus may be easily treated.

Consequently the probability of populating any given final state in a reaction can be expressed as the product of two terms. The first is the

probability that the compound nucleus will be formed and the second is the relative probability of decay into the reaction channel of interest compared with the decay into any other reaction channel allowable by kinematics. The resulting cross section is therefore expressed in the channel spin representation

$$\sigma_{\alpha\alpha'} = \frac{\pi}{k_\alpha^2} \sum_J^\pi \frac{2J+1}{(2S_A+1)(2S_a+1)} \cdot \frac{\sum_{S\ell} T_{\ell SJ}^{(\alpha)} \sum_{S'\ell'} T_{\ell'S'J}^{(\alpha')}}{\sum_{S''\ell''} T_{\ell''S''J}^{(\alpha'')}}$$

The random phase of the collision matrix components together with conservation of angular momentum and parity, reciprocity of the cross section, and the use of the optical model for compound nuclear formation is the complete statement of statistical compound nuclear model.

2.4 The γ-ray Angular Distribution

If the initial state of interest in the residual nucleus B, represented by $|J_1 M_1\rangle$, decays to a final state $|J_2 M_2\rangle$ the probability amplitude for the emission of a photon with wave vector $\vec{k}$ and circular polarization q is given by (Ro 67)

$$A^q_{M_1 M_2}(k) = \left(\frac{k}{2\pi\hbar}\right)^{\frac{1}{2}} \sum_{LM\pi} q^\pi \langle J_1 M_1 | T_{LM}^{<\pi>} | J_2 M_2 \rangle D^L_{Mq}(R) \qquad (1)$$

where the interaction $T_{LM}^{<\pi>}$ can be expressed in terms of the electromagnetic multipole operators; the superscript $<\pi>$ indicates an electric multipole

operator for $\pi = 0$ and magnetic operator for $\pi = 1$, the quantity q describes circular polarization and takes values ± 1. The $D^{L}_{Mq}(R)$ matrix, the rotation matrix, describes a rotation that projects the propagation vector $\vec{k}$ onto the z-axis. If the spin orientation of the state J_2 is not observed then in order to determine the total transition probability an incoherent sum over M_2 must be taken; that is $P^{q}_{M_1}(k)$, the probability for emission of a photon along $\vec{k}$ with polarization q from the initial state $|J_1 M_1>$ becomes

$$P^{q}_{M_1}(k) \sim \sum_{M_2} |A^{q}_{M_1 M_2}(k)|^2 \tag{2}$$

Since the radiating system is in a cylindrically symmetric environment the total radiative probability for photons of momentum $\vec{k}$ is obtained by weighing each $P^{q}_{M_1}(k)$ with the population parameter $w(M_1)$ of the magnetic substate M_1.

$$P^{q}(k) = \sum_{M_1} w(M_1) \sum_{M_2} |A^{q}_{M_1 M_2}(k)|^2 \tag{3}$$

The angular distribution formula for the emission of photons from a state J_1 to a state J_2 is obtained by the expansion of (3), (Ro 67).

$$\begin{aligned} W(\theta) = P^{q}(k) = \frac{k}{2\pi\hbar} \sum_{M_1} w(M_1) \sum_{KLL'\pi\pi'} & (LL'q-q|Ko) \\ \times \sum_{M_1 M} & (-1)^{q-M} (LL'M-M|Ko)\ (J_2 L M_2 M|J_1 M_1)\ (J_2 L' M_2 M|J_1 M_1) \\ \times & P_K(\cos\theta) q^{\pi+\pi'} <J_1\|T_L^{<\pi>}\|J_2> <J_1\|T_{L'}^{<\pi>}\|J_2>^* \end{aligned} \tag{4}$$

If this expression is now integrated over all possible directions of $\vec{k}$ and summed over q the total transition probability per unit time, or the reciprocal lifetime, of a state $|J_1 M_1>$ for gamma decay is obtained.

$$\tau^{-1} = \frac{4k}{\hbar} \sum_{L\pi} |<J_1||T_L^{<\pi>}||J_2>|^2/(2L+1) \tag{5}$$

Since the electromagnetic interaction can be expressed as

$$T_L^{<\pi>} = \alpha_L^{<\pi>} G_L^{<\pi>}$$

where $\alpha_L^{<\pi>}$ is the statistical multipole expansion coefficient and $G_L^{<\pi>}$ contains the electromagnetic multipole operators, equation (4) can be expressed as

$$\tau^{-1} = \frac{2}{\hbar} \sum_{L\pi} \frac{L+1}{L[(2L+1)!!]^2} \cdot k^{2L+1} \frac{|<J_1||G_L^{<\pi>}||J_2>|^2}{2L+1} \tag{6}$$

The angular distribution formula (4) can be expressed in terms of more suitable coefficients (c.f. Rose and Brink).

$$W(\theta) = \frac{k}{2\pi\hbar} \sum_{LL'\pi\pi'K} B_K(J_1)\, R_K^q(LL'J_1J_2) P_K(\cos\theta) q^{\pi+\pi'}$$

$$\times \frac{<J_1||T_L^{<\pi>}||J_2>}{(2L+1)^{\frac{1}{2}}} \quad \frac{<J_1||T_{L'}^{<\pi'>}||J_2>^*}{(2L'+1)^{\frac{1}{2}}} \tag{7}$$

where $R_K^q(LL'J_1J_2) = (-1)^{q+J_1-J_2+L'-L-K}(2J_1+1)^{\frac{1}{2}}\,(2L+1)^{\frac{1}{2}}\,(2L'+1)^{\frac{1}{2}}$

$$\times (LL'q-q|Ko)\, W(J_1J_1LL';KJ_2)$$

and $B_K(J_1) = \sum_{M_1} w(M_1)\ (-1)^{J_1-M_1}(2J_1+1)^{\frac{1}{2}}\ (J_1 J_1 M_1 -M_1 | Ko)$

For the specific case where circular polarization is unobserved equation (7) becomes

$$W(\theta) = \frac{k}{2\pi\hbar} \sum_{LL'\pi\pi'K} B_K(J_1)\ R_K(LL'J_1J_2)\ P_K(\cos\theta)$$

$$x\ \{1+(-1)^{L+L'+\pi+\pi'-K}\}\ \frac{\langle J_1 \| T_L^{<\pi>} \| J_2\rangle}{(2L+1)^{\frac{1}{2}}}\ \frac{\langle J_1 \| T_{L'}^{<\pi'>} \| J_2\rangle^*}{(2L'+1)^{\frac{1}{2}}} \quad (8)$$

In equation (8) the reduced matrix elements are divided by factors of $(2L+1)^{-\frac{1}{2}}$ consequently the modulus of the quantity $\langle J_1 \| T_L^{<\pi>} \| J_2\rangle/(2L+1)$ may be considered as the square root of the partial radiative width for γ-rays of character $(L\pi)$. The angular distribution of the photons emitted in the decay of state $|J_1 M_1\rangle$ can be seen to be dependent primarily on the population parameters of the magnetic substates $w(M_1)$ of the initial state, and reduced matrix elements. The remaining factors only describe the geometry of the decay and are not dependent on the physical processes involved.

The reduced matrix elements are of prime importance as they contain the nuclear information. They may be calculated directly from a nuclear model, which gives eigenfunctions for the states J_1 and J_2. Experimentally, the sum of their square moduli can be obtained from a lifetime measurement and their ratio can be determined from angular distribution measurements. In particular, for angular distribution measurements, the

mixing ratio, $\delta_L^{<\pi>}$, is introduced;

$$\delta_L^{<\pi>} = \frac{\langle J_1 \| T_L^{<\pi>} \| J_2 \rangle / (2L+1)^{\frac{1}{2}}}{\langle J_1 \| T_{\underline{L}}^{<\pi>} \| J_2 \rangle / (2\underline{L}+1)^{\frac{1}{2}}}$$

where $\underline{L}$ refers to the lowest-order multipolarity occurring in the transition J_1 to J_2 and L another allowed multipolarity in the decay of J_1 to J_2. Providing that the electromagnetic multipole operator, $T_L^{<\pi>}$, and the eigenfunctions $|J\ M>$ are invariant under time reversal the mixing ratio will be real (Lo 51); the sign of the mixing ratio is dependent on the relative phase of the matrix elements. The angular distribution can now be expressed in terms of these multipole mixing ratios (Ro 67).

$$W(\theta) = \sum_{LL'\pi\pi'K} B_K(J_1)\ R_K(LL'J_1J_2)\ P_K(\cos\theta)\{\frac{1+(-1)^{L+L'+\pi+\pi'-K}}{2}\}$$

$$\times\ \delta_L^{<\pi>}\ \delta_{L'}^{<\pi>} / \sum_{L\pi} |\delta_L^{<\pi>}|^2 \qquad (9)$$

This angular distribution formula describes the case where circular polarization is not observed and the initial state may be polarized or aligned and need not have definite parity. If the initial and final nuclear states have definite parity only the even order K terms will contribute to the distribution. Since the electromagnetic interaction conserves parity the sum over $LL'\pi\pi'$ need not run independently over all possible values because there is now a fixed relation between the allowed values of L and π. If J_1 and J_2 are of the same parity only even values of L will occur for the electric interaction ($\pi = 0$), and only odd values will occur for the magnetic interaction ($\pi = 1$). The restrictions on the possible

L values are reversed for the case where the two states J_1 and J_2 have opposite parity. Where there is no change in parity between J_1 and J_2, only M1, E2, M3, etc. are allowed whereas E1, M2, E3, etc., are allowed for the case of parity change. Consequently the value of $L + L' + \pi + \pi'$ will always be even and hence only even values of K will be observed in the distribution. The odd order K terms will be observed in the angular distribution, when circular polarization is not observed, only if the states J_1 and J_2 do not have definite paiity. The angular distribution takes the form

$$W(\theta) = \sum_{\substack{(L\pi)(L'\pi') \\ K = \text{even}}} B_K(J_1) R_K(LL'J_1J_2) \frac{\delta_L^{<\pi>} \delta_{L'}^{<\pi>}}{\sum_L |\delta_L^{<\pi>}|^2} P_K(\cos\theta) \quad (10)$$

where the sum of $(L\pi)$ is over all possible multipoles consistent with conservation of angular momentum and parity

$$|J_1 - J_2| \leq L \leq J_1 + J_2$$

In general, only the two lowest multipolarities $\underline{L}$ and L' are considered to contribute to the distribution so that

$$W(\theta) = \sum_{K \text{ even}} B_K(J_1) P_K(\cos\theta) \times \frac{\{R_K(\underline{L}\underline{L}J_1J_2) + 2\delta R_K(\underline{L}L'J_1J_2) + \delta^2 R_K(L'L'J_1J_2)\}}{1 + \delta^2} \quad (11)$$

2.5 The (p,nγ) Reaction

The alignment in a (p,nγ) reaction will be considered in two parts: the formation of the compound nuclear state, and the subsequent decay of this state. If the beam direction is chosen as the quantization axis the population parameters of the intermediate state, in the channel spin representation, will be proportional to the quantity

$$W(M_{int}) \sim (S\ell M_1 o | J_{int} M_{int})^2$$

where S is the channel spin with projection M_1 and ℓ is the angular momentum of the incident partial wave. If more than one channel spin can contribute to the formation of J_1 the contributions from each channel are added incoherently

$$W(M_{int}) \sim \sum_S (S\ell M_1 o | J_{int} M_{int})^2 T_S$$

where T_S is a channel spin intensity factor. If two partial waves contribute to the formation of J_{int} the population parameters will become proportional to

$$W(M_{int}) \sim \sum_S | (S\ell M_1 o | J_{int} M_{int}) A_\ell +$$

$$(S\ell' M_1 o | J_{int} M_{int}) A_{\ell'} |^2 T_S$$

where A_ℓ and $A_{\ell'}$ are the amplitudes of the partial waves ℓ and ℓ'

which couple with the channel spin S to form the intermediate state J_{int}. These wave amplitudes can be expressed by the transmission coefficients and hence the population parameters for the intermediate state will be expressed in terms of spin factors, Clebsch-Gordan coefficients and the projectile's transmission coefficients. (For protons incident on even nuclei only one value of ℓ and S (= 1/2) contribute to J_{int}.) The state J_1 formed after neutron emission will thus have population parameters expressed as a product of Clebsch-Gordan and Racah coefficients and a penetrability term τ, where τ is the probability of the reaction occurring and is expressed in terms of the proton and neutron transmission coefficients, i.e.

$$\tau = \frac{T^{j_p}_{\ell_p}(E_p) T^{j_n}_{\ell_n}(E_n)}{\sum T^{j}_{\ell}(E)}$$

The resulting expression for the angular distribution becomes

$$W(\theta) = \frac{\lambda^2}{4} \sum (-1)^{J_0 + J_2 - s_p - j_n - 1} (2J_{int}+1)(2\ell_p+1)(2j_p+1)$$

$$\times (2J_1+1)(2J_0+1)^{-1}(2s_p+1)^{-1}(\ell_p \ell_p oo|Ko)$$

$$\times W(\ell_p \ell_p j_p j_p; K s_p) W(j_p j_p J_{int} J_{int}; K J_0)$$

$$\times W(J_{int} J_{int} J_1 J_1; K j_n) \tau M(\delta) P_K(\cos\theta) \qquad (12)$$

where $M(\theta) = \frac{M(\underline{L}\,\underline{L}) + 2\delta M(\underline{L}L') + \delta^2 M(L'L')}{1 + \delta^2}$

and $M(\underline{L}L') = (-1)^{J_2-J_1+L-L'-K}(2J_1+1)^{-\frac{1}{2}} R_K(LL'J_1J_2)$

The angular distribution is normally expressed in the simplified form

$$W(\theta) = \sum_{K \text{ even}} a_K P_K(\cos\theta)$$

The coefficients for all possible spin sequences and multipolarities are calculated in the computer programme MANDY, written by Sheldon and Strang (Sh 69). The transmission coefficients were calculated using several sets of optical model parameters with the help of the programme Hauser (Da 01).

The dependence of the predicted a_K coefficients on the transmission coefficients is discussed in the appendix for various transition spin sequences and values of the multipole mixing ratio.

CHAPTER 3

EXPERIMENTAL PROCEDURE

3.1 Apparatus

Protons, accelerated by the University of Alberta 5.5 MeV van de Graaff, were used to bombard a thick nickel target (enriched to 96% in ^{64}Ni). Following terminal analysis and focussing the beam was bent through 90° by an analyzing magnet and defined on the target by a double-focussing quadrupole pair and a collimator of diameter 0.15 cm. A 5 cm diameter cylindrical piece of Perspex faced at 30° with respect to the beam direction was used as a target holder. A 1.3 cm diameter hole through the centre of the Perspex allowed beam passage. The target was fastened to the holder with a 2 mm aluminum plate, which also served as a charge collector. The targets were prepared by mixing a small amount of isotope into a glue formed by dissolving polyurethane in benzene and smearing the mixture onto a .112 mm thick tantalum backing.

Since the excited states of interest in ^{64}Cu known were to be of low spin the proton bombarding energies were chosen near threshold for neutron population so as to ensure minimal de-alignment of the compound nuclear state. At the same time care was taken to ensure that the proton bombarding energies would produce sufficiently high gamma-ray yields. The state of interest in ^{64}Cu was excited at less than 210 keV above threshold.

The gamma-ray angular distributions were observed using a 15 cc Ge(Li) detector which could be positioned at angles between 0° and 90° to the beam direction. A fixed 6 cc Ge(Li) detector was used as a monitor. The

resolution obtained with the Ge(Li) detectors was typically 3.5 keV FWHM for the 1.332 MeV ^{60}Co full energy peak. Signals from the 15 cc Ge(Li) detector were sent into a pre-amplifier[†]-amplifier[††] assembly and then into an analogue-to-digital converter[†††]. The signals from the amplifier were also sent through an integral discriminator[*] into a rate meter[**]. The signals from the 6 cc Ge(Li) were also fed into a pre-amplifier[°]-amplifier[°°] assembly and sent to an analogue-to-digital converter[†††]. The signals from the analogue-to-digital converters were sent to an SDS 920 computer which was equipped with display and light pen.

3.2 Acquisition of Data and Analysis

Following preliminary investigation of the gamma ray yield and the decay scheme of the low-lying states of ^{64}Cu, the gamma-ray intensity at five angles (0, 30, 45, 60 and 90 degrees) were measured for proton bombarding energies of 2.78 MeV, 2.95 MeV and 3.25 MeV. All angles were repeated at least once.

[†] Canberra model 1408 A/B

[††] Tennelec model TC203 BLR Linear Amplifier

[†††] Technical Measurements Corporation (TMC) model 217 A

[°] Nuclear diode model 101A

[°°] Canberra model 1417 B Spectroscopy amplifier

[*] Ortec model 421

[**] Ortec model 441

For each gamma ray angular distribution the gain settings of the amplifiers were adjusted to isolate the gamma rays of interest. The beam current was adjusted so that the gamma-ray counting rate at the different angles was constant. For most of the angular distributions the counting rate was kept at ~ 7000 counts/s. This required a beam current of approximately 0.5 μA; such conditions produced an approximate live time of 80% in the analogue-to-digital converters.

Gamma rays decaying from ^{64}Cu were determined by observing new transitions as the bombarding energy was increased, resulting in neutron population of the higher excited states, and by fitting them consistently into a decay scheme of the known levels of ^{64}Cu (Sh 68). The polyurethane-benzene target matrix did not yield any contaminant gamma rays because of the large negative Q values for the proton induced reaction on carbon, oxygen, and nitrogen (Nu 64). The observed γ-rays not attributed to ^{64}Cu were

i) the 1.388 MeV gamma ray and its corresponding double escape peak from ^{64}Ni(p,p'γ)

ii) the 0.770 MeV gamma ray decaying from the first excited state of ^{65}Cu following the ^{64}Ni(p,γ) reaction

iii) the 0.440 MeV and 1.63 MeV gamma rays resulting from the ^{23}Na (p,p'γ) and ^{23}Na(p,$\alpha\gamma$)^{20}Ne reactions respectively.

In addition to these contaminant gamma rays, neutrons from the (p,n) reaction interacting with the germanium in the detector resulted in the ^{74,72}Ge(n,n'γ) reactions and produced gamma rays of 0.597 and 0.693 MeV.

Similarly gamma rays at 0.136 MeV and 0.302 MeV were attributed to the $^{181}Ta(n,n'\gamma)$ resulting from neutron interaction with the tantalum backing.

The strong 0.278 MeV gamma ray from the second excited state of ^{64}Cu was used as a monitor for the angular distributions measured at proton bombarding energy of 2.95 MeV and 3.25 MeV. For the γ-ray angular distribution studied at 2.78 MeV bombarding energy however, the 0.159 MeV gamma ray from the first excited state of ^{64}Cu, was used; the yield of the 0.278 MeV gamma ray being too weak to give good statistics. A typical gamma-ray spectrum is shown in figure 1.

During the experiment the intensities of the γ-rays were obtained by summing over the full energy peaks and subtracting the background directly from the computer display. More accurate γ-ray intensities were obtained for the final analysis using a computerized plot programme (Da 01), in which the background is calculated and subtracted using a subroutine written by Tepel (Te 66).

The experimental angular distributions were fitted using least squares to the expansion $w(\theta) = a_0[1 + a_2P_2(\cos\theta) + a_4P_4(\cos\theta)]$, (Dr 70), with the Legendre coefficients a_0, a_2, and a_4 treated as adjustable parameters. The experimental a_2 and a_4 coefficients were compared to the theoretical predictions of the compound nuclear statistical model (Sh 66) for various spin sequences and multipole mixing ratios.

The optical model parameters of Rosen (Ro 66), Perey (Pe 63), and O'Brien (OB 67) were used to determine the transmission coefficients for the proton, neutron and alpha compound nuclear decay channels respectively.

Figure 1 A typical gamma-ray spectrum observed at proton bombarding energy of 3.25 MeV and detector angle 55°.

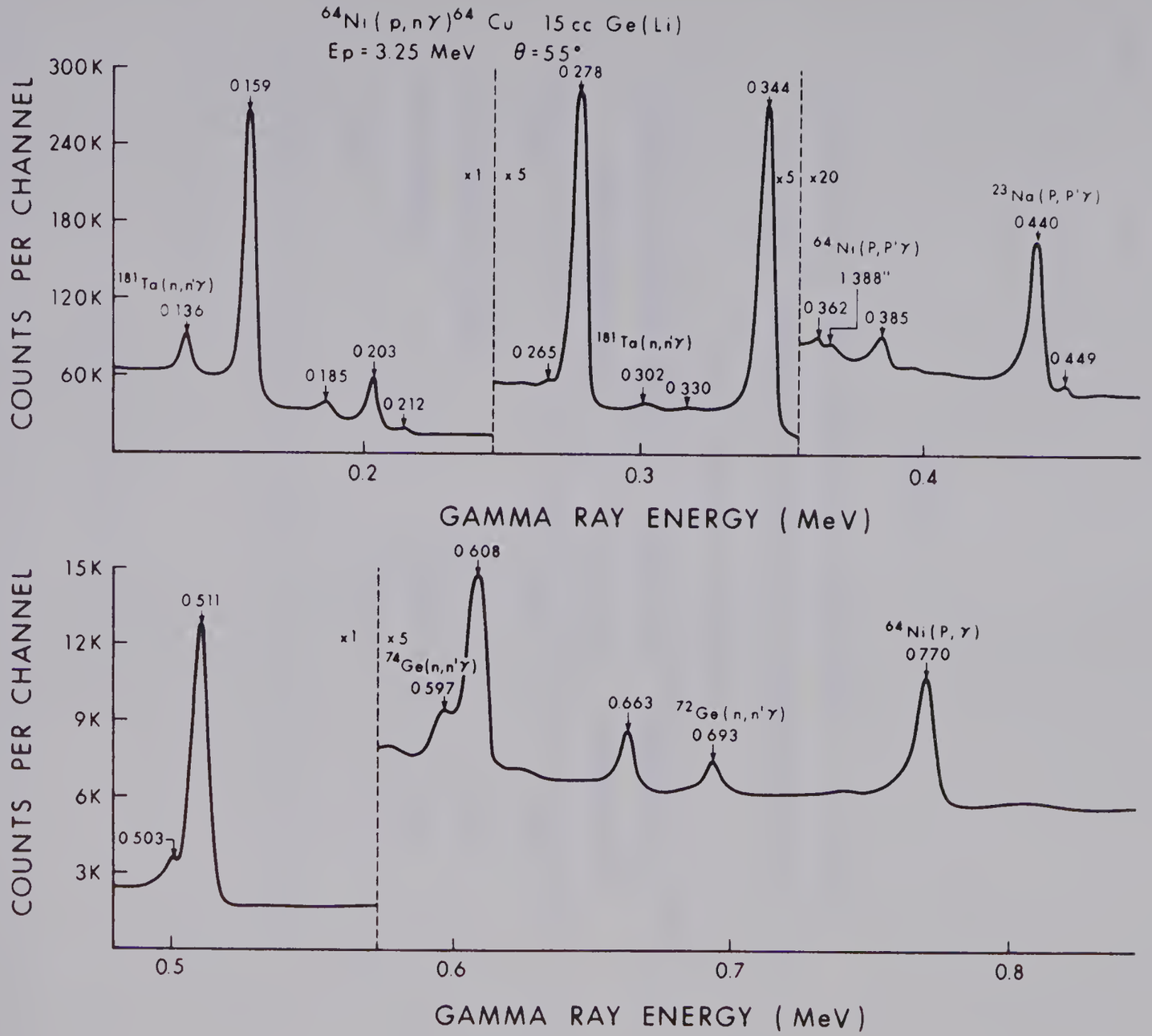
^{64}Ni(p,nγ)^{64}Cu 15 cc Ge(Li)
Ep = 3.25 MeV θ = 55°
COUNTS PER CHANNEL
300K
240K
180K
120K
60K
0.159
0.278
0.344
x1
x5
x5
x20
^{23}Na(P,P'γ)
0.440
^{64}Ni(P,P'γ)
1.388"
0.362
0.385
^{181}Ta(n,n'γ)
0.136
0.203
0.185
0.212
0.265
^{181}Ta(n,n'γ)
0.302
0.330
0.449
0.2
0.3
0.4
GAMMA RAY ENERGY (MeV)
COUNTS PER CHANNEL
15K
12K
9K
6K
3K
0.608
0.511
x1
x5
^{74}Ge(n,n'γ)
0.597
^{64}Ni(P,γ)
0.770
0.663
^{72}Ge(n,n'γ)
0.693
0.503
0.5
0.6
0.7
0.8
GAMMA RAY ENERGY (MeV)

Figure 1

TABLE 2

Sensitivity of the Predicted a_k Coefficients to the Ratio $T_{\ell=1} / T_{\ell=0}$ Obtained at 100 keV Above Threshold for a 2^+ to 1^+ Pure M_1 Transition

Source of Neutron Optical Model Parameters	Ratio of $T_{\ell=1}/T_{\ell=0}$	Predicted a_2 Coefficient
Perey	0.0442	-.345
Bjorklund-Fernbach	0.0736	-.314
Perey-Buck	0.0542	-.331
Rosen	0.0510	-.323

Additional sets of neutron transmission coefficients were obtained by substituting the neutron optical model parameters of Perey-Buck (PB 62), Bjorklund-Fernbach (BF 58), and Gurd (Gu 68) in the Hauser-Feshbach programme. These sets were used as a means of checking the sensitivity of the predicted Legendre coefficients to the transmission coefficients. Although the absolute magnitudes of the transmission coefficients differed by a factor of three the relative quantities $T_\ell = 1/T_\ell = 0$ agreed to within 40%. The compound statistical model predictions were extremely insensitive to these differences (see table 2).

As an additional check of the sensitivity of the compound nuclear statistical model to the transmission coefficients the proton (Ro 66,Co 62) and alpha-particle transmission coefficients were varied. A negligible change in the calculated Legendre coefficients resulted.

For some of the more anisotropic gamma rays, spin assignments could be made by superimposing the experimental Legendre coefficients directly onto the predicted a_2-a_4 multipole ellipses (see appendix). This however gave no indication of the goodness of fit for the other possible spin assignments and in order to determine whether or not a unique spin assignment had been found χ^2 calculations were performed (Gr 70). The quantity χ^2 defined by

$$\chi^2 = \frac{1}{n-1} \sum_{i=1}^{n} \frac{(W(\theta_i) - Y(\theta_i))^2}{EY(\theta_i)^2}$$

where $W(\theta_i)$ and $Y(\theta_i)$ are the predicted and experimental γ-ray intensities at angle θ_i respectively, $EY(\theta_i)$ is the statistical uncertainty in the

experimental intensity measurement at θ_i, and n is the number of degrees of freedom. χ^2 was calculated using the predicted a_2 and a_4 coefficients for all possible spin sequences and multipole mixing ratios. Spin assignments which fell outside the limits of χ^2 at the 0.1% confidence limit were rejected, implying that there was only one chance in a thousand that the correct spin assignment was rejected.

These χ^2 plots, together with the angular distributions, are shown in the next section.

CHAPTER 4

RESULTS

4.1 Determination of Gamma-Ray Energies

For determination of the gamma ray energies a linear calibration curve was constructed using ^{57}Co, ^{54}Mn, ^{22}Na and ^{60}Co sources. Since the energies of the gamma rays of interest in ^{64}Cu lay within the calibrated region the gamma ray energies of ^{64}Cu could be interpolated and are expected to be accurate within 1 keV. The energies of ground state transitions were checked whenever possible with the energy sum of the cascades via intermediate levels. These agreed within 1 keV.

4.2 Branching Ratio Measurements

The γ-ray branching ratios were determined from all observed gamma ray intensities observed at 55° at a proton bombarding energy of 3.25 MeV. Since the a_4 coefficients for the distributions were small (< .05) the measured values of the A_0 coefficients could be determined to within 2%. The relative efficiency of the 15 cc Ge(Li) detector, used in the branching ratio measurement, was determined using the ^{57}Co, ^{54}Mn, ^{137}Cs, ^{22}Na and ^{60}Co sources. The absence of gamma rays in the energy range 200 to 600 keV introduced an additional 2% error. Consequently the branching ratios should be accurate within $\pm$ 4%. The efficiency curve is shown in figure 2.

Figure 2 Relative photopeak efficiency of the 15 cc Ge(Li) for a range of gamma ray energies from 0.1 to 1.3 MeV.

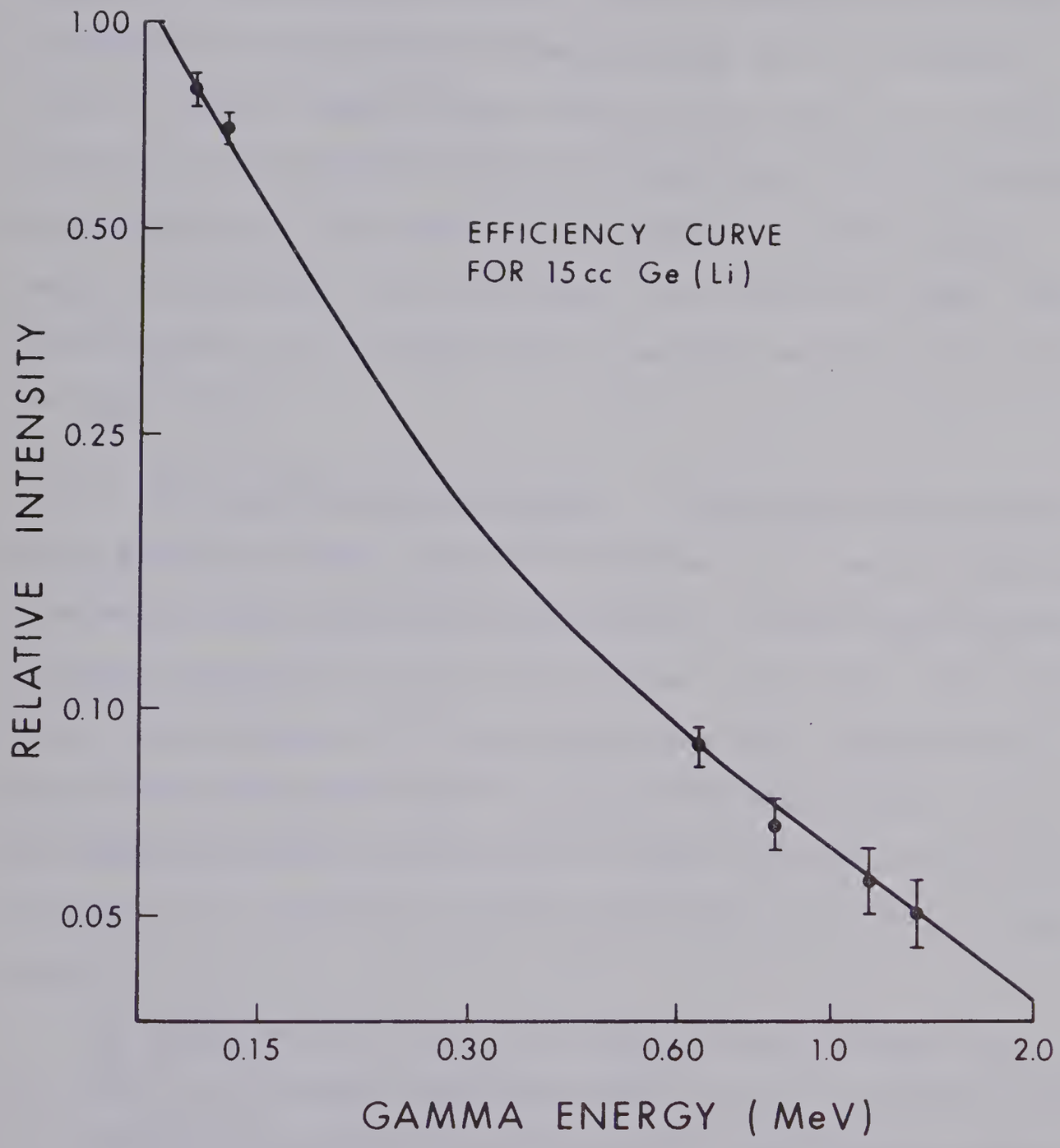
1.00
0.50
0.25
0.10
0.05
RELATIVE INTENSITY
EFFICIENCY CURVE
FOR 15 cc Ge (Li)
0.15
0.30
0.60
1.0
2.0
GAMMA ENERGY (MeV)

Figure 2

4.3 Experimental Results and Deductions

The gamma ray branching ratios, a_k coefficients, deduced spins and mixing ratios are summarized together with the recently published spin assignments and mixing ratios of Davidson et al. (Da 70) in tables 3, 4 and 5. Figure 3 shows the decay scheme for the levels up to 700 keV excitation in ^{64}Cu together with the branching ratios and spin assignments as determined from this present study. Figures 4 to 9 show selected angular distributions with corresponding 'best fits' and χ^2 peaks. The sign convention for the mixing ratio is consistent with that used by Rose and Brink (Ro 67).

4.3.1 The 0.159 and 0.278 MeV levels These levels decay directly to the ground state whose spin-parity assignment of 1^+ has been determined from magnetic moment measurements (Le 54,Do 66). These transitions were extremely anisotropic (a_2 was -0.36 ± 0.02 and -0.40 ± 0.01 respectively); unique spin assignments of 2^+ were made in each case. The parities of these levels were deduced from ^{63}Cu(d,p) and ^{66}Zn(d,α) studies (Pa 69) for which the stripping cross-section for both levels was characteristic of an $\ell_n = 1$ or 3 transfer in the (d,p) case and by an L = 0 or 2 in the (d,α).

The mixing ratio for the 159 keV gamma ray was determined to be $\delta = -0.07 \pm 0.02$; however, the insensitivity of the χ^2 calculation to the a_4 coefficient resulted in the determination of another possible value for δ, namely $\delta = -2.39 \, ^{+0.15}_{-0.24}$.

These mixing ratios together with the lifetime measurement of $\tau < 0.3$

nsec determined by du Toit and Bollinger (To 61) indicate an E2 enhancement of approximately 3 W.U. and 700 W.U. respectively. However as the second mixing ratio corresponds to a predicted $a_4 = 0.18$ as compared to the experimental value $a_4 = -0.01 \pm 0.02$, this value of δ can probably be excluded.

The mixing ratios for the 278 keV gamma ray were determined to be $\delta = -0.16 \pm 0.02$ and $\delta = -1.69 \begin{smallmatrix} +0.14 \\ -0.23 \end{smallmatrix}$. The lifetime measurement $\tau < 0.3$ nsec (To 61) as a result indicates an E2 enhancement of approximately 15 W.U. and 70 W.U. respectively.

Since a_4(theory) = 0.11 as compared to a_4(exp) = 0.04 ± 0.01 the second value of the mixing ratio can probably be excluded.

The 159 keV and 278 keV gamma rays can probably be considered as almost pure M_1 transitions.

The distributions with corresponding "best fits" and χ^2 plots are shown in figures 4 and 5.

4.3.2 The 0.344 MeV level This state decays 96% via a 344 keV ground state transition and 4% via a 185 keV gamma ray to the 159 keV state. The angular distributions for both of these gamma rays were measured at proton bombarding energy of 2.95 MeV and were found to be only slightly anisotropic (a_2 was 0.06 ± 0.02 and 0.08 ± 0.04 respectively). When the distribution for the 344 keV gamma ray was compared to theoretical predictions (figure 6) spin assignments of 1^+ and 2^+ were found to be equally probable. Parity was deduced from the ^{63}Cu(d,p) stripping investigations referred to earlier (Pa 69), the

cross section for the 344 level being characteristic of a $\ell_n = 1$ transfer. The mixing ratios were determined to be $\delta = 0.23 \pm 0.09$ or $-9.14\ ^{+0.86}_{-1.62}$ for the 2^+ assignment and $-0.09 \leq \delta \leq \infty$ for the 1^+ assignment.

4.3.3 The 0.362 MeV level The 362 keV level decays primarily (93%) via a 203 keV gamma ray to the 159 keV level. A weak 362 keV gamma ray (7% of the total intensity) is attributed to a direct ground state transition. The angular distribution for the 203 keV gamma ray was extremely anisotropic ($a_2 = -0.45 \pm 0.03$); when compared to the theoretical compound nuclear predications a unique spin of 3^+ was assigned (figure 7). [The choice of parity was based on the results of the (d,p) and (d,α) experiments previously mentioned]. The mixing ratio was determined to be $\delta = -0.08 \pm 0.02$ indicating an almost pure M_1 transition.

Angular distributions to investigate the spin of the 574 keV level were not possible because of the low intensity of the 212 keV gamma ray.

4.3.4 The 0.608 MeV level The ground state transition is the predominant decay (80%) of this level. Weak transitions, representing 8%, 9% and 3% of the total intensity occur to the 344 keV, 278 keV and 159 keV levels respectively. The measured a_2 coefficient for the angular distribution of the 608 keV gamma ray was -0.36 ± 0.01. Comparison with theoretical predictions resulted in a unique 2^+ spin

assignment. In accord with the determined $\ell_n = 1$ transfer for the $^{63}Cu(d,p)$ stripping cross-section to this level positive parity was assumed for the spin assignment. Two possible values for the mixing ratio were determined from the χ^2 calculations (figure 8), i.e. $\delta = -0.07 \pm 0.01$ and $\delta = -2.14 \begin{smallmatrix}+0.18\\-0.26\end{smallmatrix}$. Since the latter value corresponds to a predicted $a_4 = 0.14$, as compared to the experimental value of $a_4 = 0.01 \pm 0.01$, this value can probably be excluded and the gamma ray considered as an almost pure M_1 transition.

4.3.5 The 0.663 MeV level This level decays 46% via a 385 keV gamma to the 278 keV level, 24% via a 504 gamma ray to the 159 keV level, and 30% to the ground state.

Although the angular distributions for the 385 keV and 663 keV gamma rays were slightly anisotropic ($a_2 = -0.07 \pm 0.03$ and 0.07 ± 0.03 respectively), indicating the unlikelihood of a 0^+ assignment, comparison of the angular distribution for the ground state transition with the theoretical predictions, based on the 0.1% χ^2 confidence limit, indicated that 0^+, 1^+, and 2^+ were all possible spin assignments (figure 9). The parity for this level was deduced from the results of the $^{63}Cu(d,p)$ investigation. No mixing ratios could be determined.

TABLE 3

Gamma Ray Branching Ratios Determined from the Present Experiment

Transition		Branching
Initial State (keV)	Final State (keV)	Ratio[†]
159	0	100
278	0	100
344	0	96
	159	4
362	0	7
	159	93
574	362	(100)
608	0	80
	159	3
	278	9
	344	8
663	0	30
	159	24
	278	46

[†]The branching ratios are expected to be accurate to within ± 4%.

TABLE 4

The Legendre Coefficients for the Fitted Angular Distribution of the More Predominant Gamma Rays Emitted in the Decay of the Low Lying States of ^{64}Cu.

Bombarding Energy E_p (MeV)	Transition	E_γ (MeV)	a_2	a_4
2.78	0.159 → 0.0	0.159	-0.36 ± 0.02	-0.01 ± 0.02
2.95	0.278 → 0.0	0.278	-0.40 ± 0.01	0.04 ± 0.01
	0.344 → 0.0	0.344	0.06 ± 0.02	-0.02 ± 0.02
	0.344 → 0.159	0.185	0.08 ± 0.04	-0.11 ± 0.05
	0.362 → 0.159	0.203	-0.45 ± 0.03	0.01 ± 0.02
3.25	0.608 → 0.0	0.608	-0.36 ± 0.01	0.01 ± 0.01
	0.663 → 0.0	0.663	0.07 ± 0.03	-0.06 ± 0.04
	0.663 → 0.278	0.385	-0.07 ± 0.03	0.00 ± 0.03

TABLE 5

Spin Assignments and Multipole Mixing Ratios Determined from the Present Work together with the Recently Published Results of Davidson et al. (Da 70)

Transition		Present Work		Davidson et al.	
Initial State (keV)	Final State (keV)	Spin Sequence	Mixing† Ratio	Spin Sequence	Mixing†† Ratio
159	0	$2^+ \rightarrow 1^+$	-0.07 ± 0.02 $(-2.39\ ^{+\ 0.15}_{-\ 0.24})$	$2^+ \rightarrow 1^+$	-0.01 ± 0.02
278	0	$2^+ \rightarrow 1^+$	-0.16 ± 0.02 $(-1.69\ ^{+\ 0.14}_{-\ 0.23})$	$2^+ \rightarrow 1^+$	-0.025 ± 0.025
344	0	$1^+ \rightarrow 1^+$	$-0.09 \leq \delta \leq \infty$	$1^+ \rightarrow 1^+$	$\delta > 0$
		$2^+ \rightarrow 1^+$	0.23 ± 0.09 $(-9.14\ ^{+\ 0.86}_{-\ 1.62})$		
362	159	$3^+ \rightarrow 2^+$	-0.08 ± 0.02	$3^+ \rightarrow 2^+$	0.040 ± 0.035
				$2^+ \rightarrow 2^+$	$.85 \leq \delta \leq 3.5$
608	0	$2^+ \rightarrow 1^+$	-0.07 ± 0.01 $(-2.14\ ^{+\ 0.18}_{-\ 0.26})$	$2^+ \rightarrow 1^+$	0.03 ± 0.03
663	0	$0^+, 1^+, 2^+ \rightarrow 1$	undetermined	$1^+ \rightarrow 1^+$	undetermined

† The spins were determined by the 0.1% χ^2 confidence limit; the sign of δ is consistent with the Rose and Brink convention.

†† The spins were determined by direct superposition of experimental a_K coefficients onto the predicted multipole ellipses; the sign of the mixing ratio is opposite the Rose and Brink convention.

Figure 3 Decay scheme for the levels up to 700 keV excitation in ^{64}Cu together with spin assignments, branching ratios and gamma ray energies.

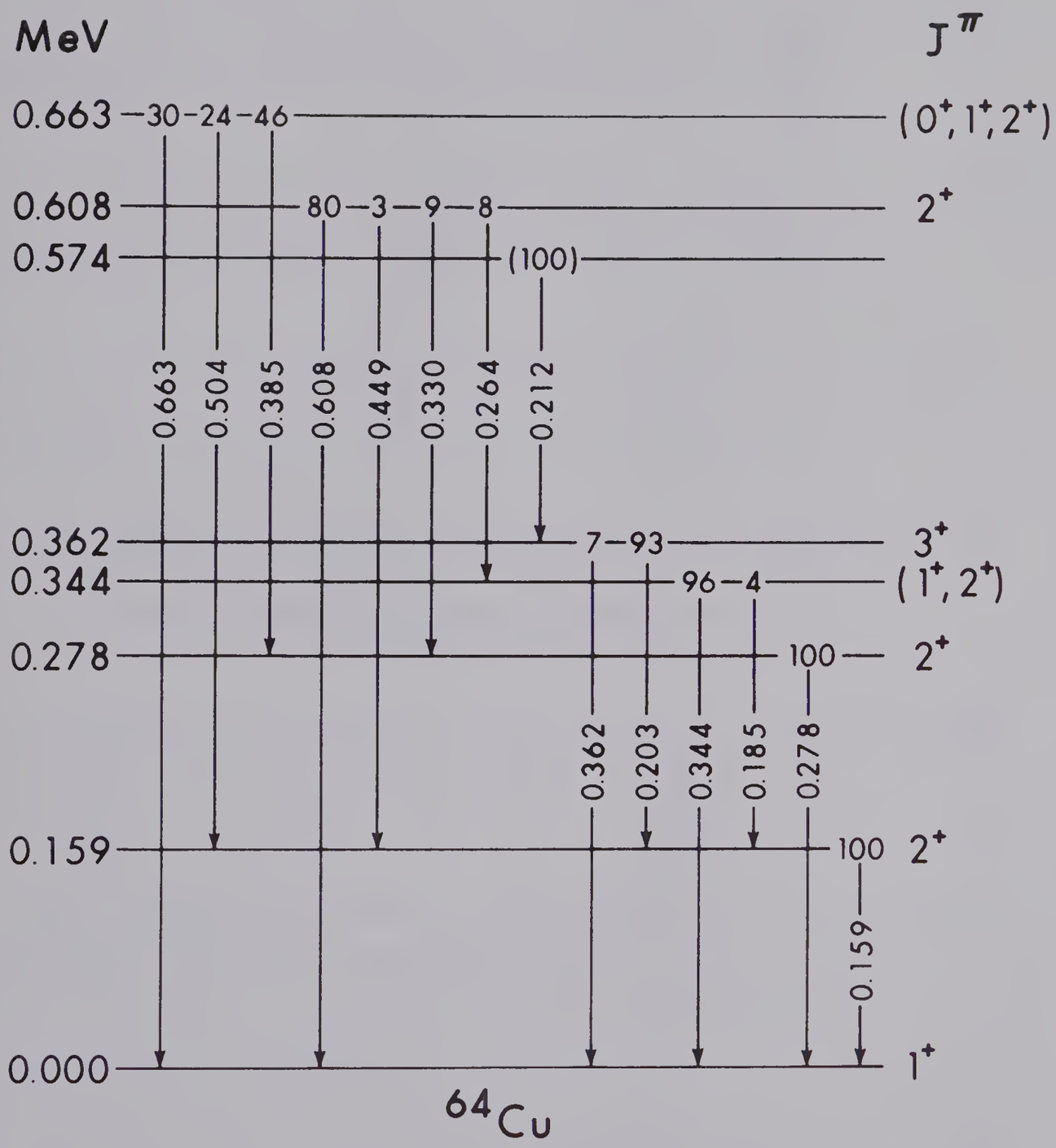
MeV
J^π
0.663
0.608
0.574
0.362
0.344
0.278
0.159
0.000
30
24
46
80
3
9
8
(100)
7
93
96
4
100
100
0.663
0.504
0.385
0.608
0.449
0.330
0.264
0.212
0.362
0.203
0.344
0.185
0.278
0.159
$(0^+, 1^+, 2^+)$
2^+
3^+
$(1^+, 2^+)$
2^+
2^+
1^+
^{64}Cu

Figure 3

Figure 4 Angular distribution with corresponding 'best fits' and χ^2 vs arc tan δ plots for the 159 keV ground state transition.

Figure 5 Angular distribution with corresponding 'best fits' and χ^2 vs arc tan δ plots for the 278 keV ground state transition.

Figure 6 Angular distribution with corresponding 'best fits' and χ^2 vs arc tan δ plots for the 344 keV ground state transition.

Figure 7 Angular distribution with corresponding 'best fits' and χ^2 vs arc tan δ plots for the 362 to 159 keV transition.

Figure 8 Angular distribution with corresponding 'best fits' and χ^2 vs arc tan δ plots for the 608 keV ground state transition.

Figure 9 Angular distribution with corresponding 'best fits' and χ^2 vs arc tan δ plots for the 663 keV ground state transition.

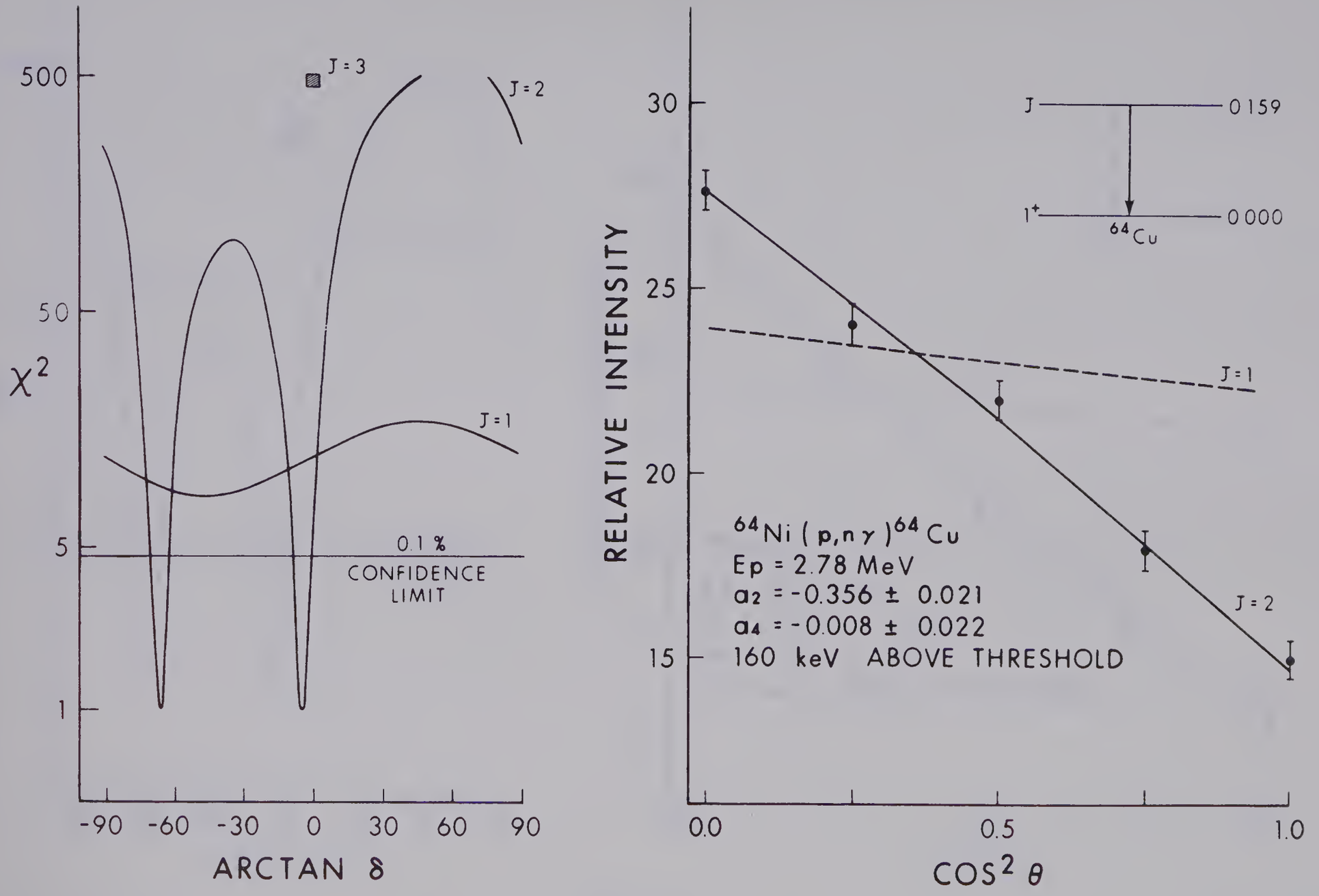
500
50
5
1
χ^2
J = 3
J = 2
J = 1
0.1 %
CONFIDENCE
LIMIT
-90 -60 -30 0 30 60 90
ARCTAN δ
30
25
20
15
RELATIVE INTENSITY
J
0 159
1+
0 000
64 Cu
64Ni (p,n γ)64 Cu
Ep = 2.78 MeV
a2 = -0.356 ± 0.021
a4 = -0.008 ± 0.022
160 keV ABOVE THRESHOLD
J = 1
J = 2
0.0
0.5
1.0
COS2 θ

Figure 4

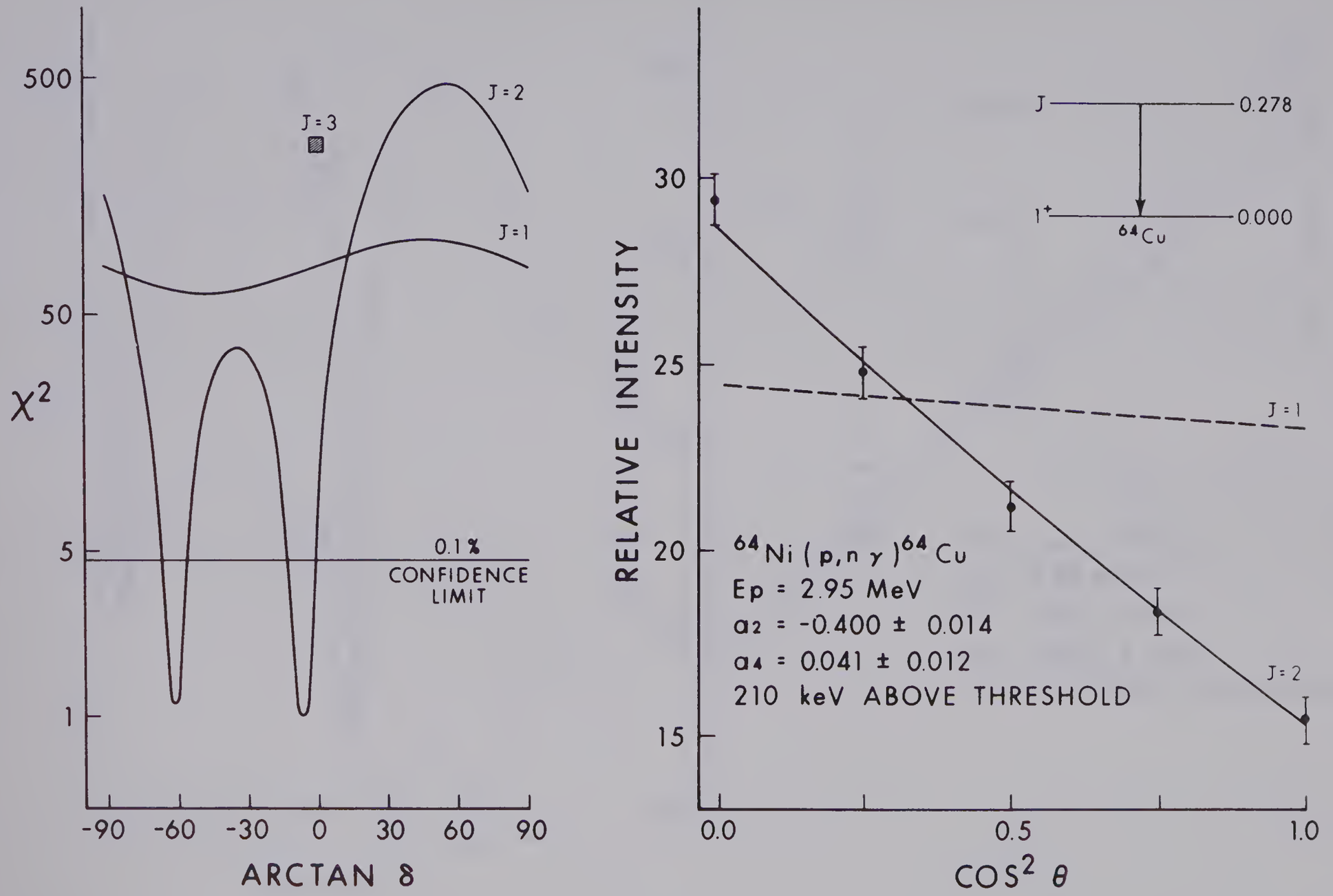
500
50
5
1
χ^2
J = 2
J = 3
J = 1
0.1 %
CONFIDENCE
LIMIT
-90 -60 -30 0 30 60 90
ARCTAN δ
RELATIVE INTENSITY
30
25
20
15
J
0.278
1+
0.000
64Cu
64Ni (p,n γ)64 Cu
Ep = 2.95 MeV
a2 = -0.400 ± 0.014
a4 = 0.041 ± 0.012
210 keV ABOVE THRESHOLD
J = 1
J = 2
0.0 0.5 1.0
COS2 θ

Figure 5

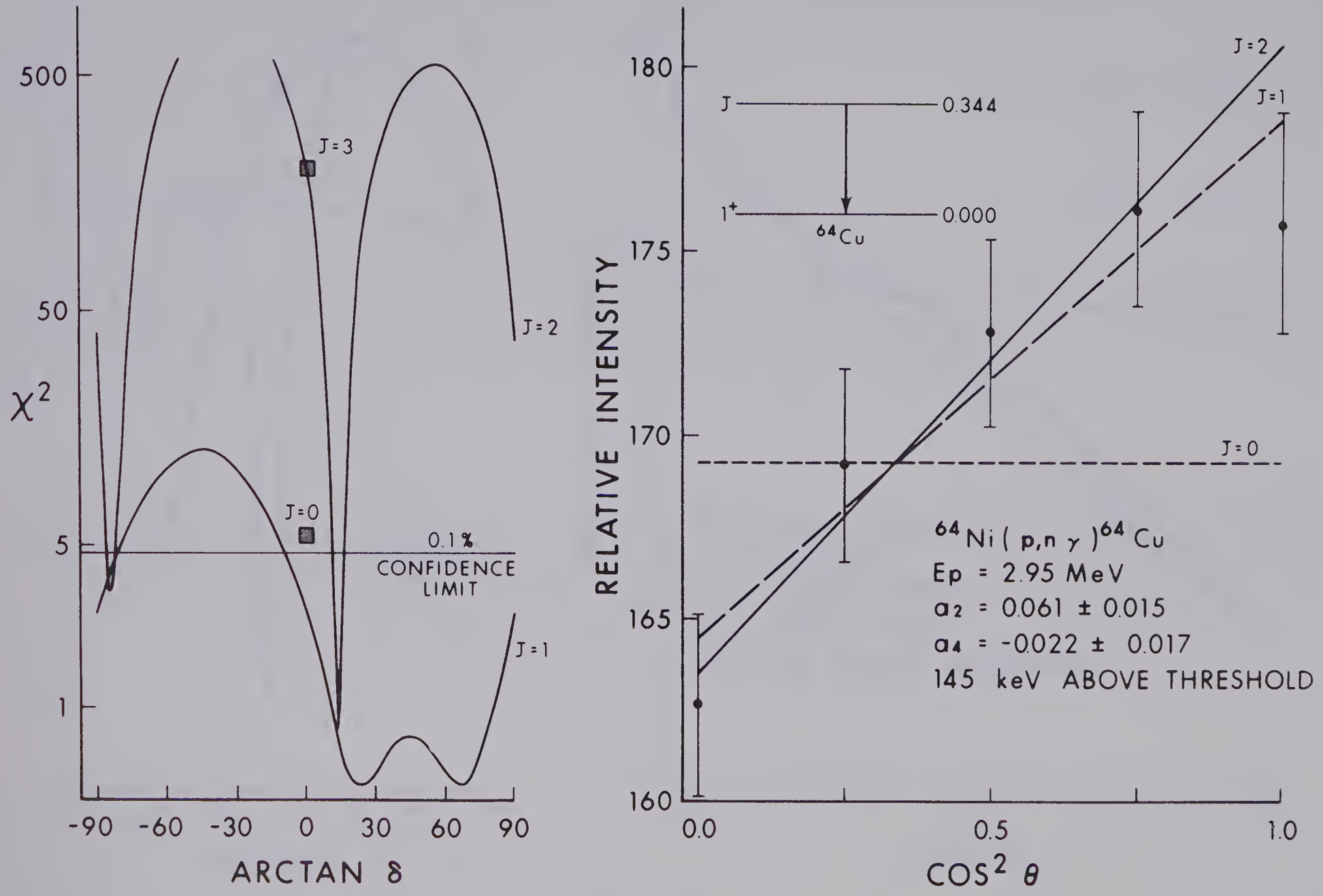
500
50
5
1
χ^2
J=3
J=2
J=0
J=1
0.1%
CONFIDENCE
LIMIT
-90 -60 -30 0 30 60 90
ARCTAN δ
180
175
170
165
160
RELATIVE INTENSITY
J
0.344
1+
0.000
64Cu
J=2
J=1
J=0
64Ni (p,n γ)64 Cu
Ep = 2.95 MeV
a2 = 0.061 ± 0.015
a4 = -0.022 ± 0.017
145 keV ABOVE THRESHOLD
0.0
0.5
1.0
COS2 θ

Figure 6

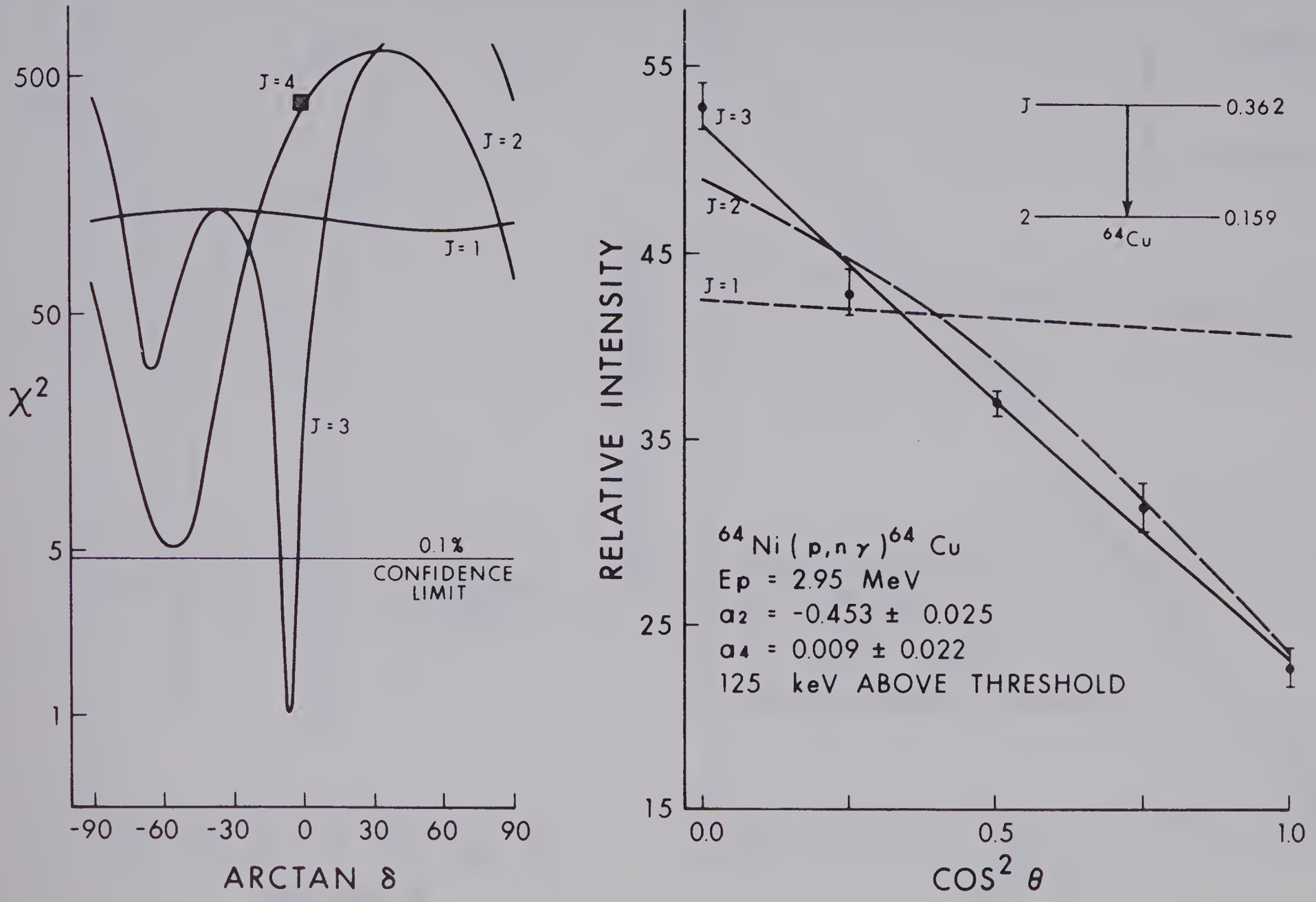
500
50
5
1
χ^2
J = 4
J = 2
J = 1
J = 3
0.1%
CONFIDENCE
LIMIT
-90 -60 -30 0 30 60 90
ARCTAN δ
55
45
35
25
15
RELATIVE INTENSITY
J = 3
J = 2
J = 1
J
0.362
2
0.159
^{64}Cu
^{64}Ni (p,n γ)^{64} Cu
Ep = 2.95 MeV
a_2 = -0.453 ± 0.025
a_4 = 0.009 ± 0.022
125 keV ABOVE THRESHOLD
0.0
0.5
1.0
COS^2 θ

Figure 7

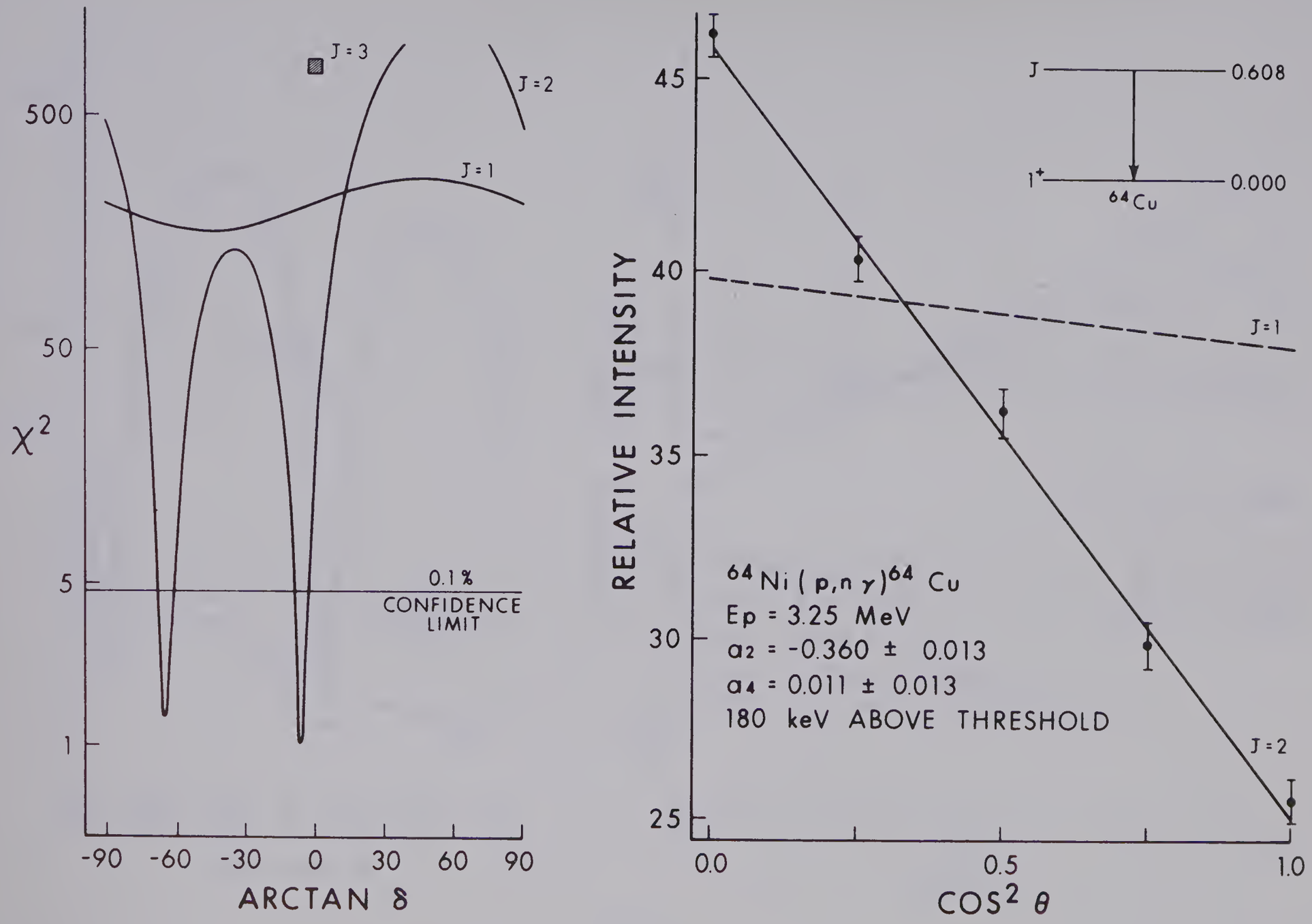
J = 3
J = 2
J = 1
500
50
5
1
χ^2
0.1 %
CONFIDENCE
LIMIT
-90 -60 -30 0 30 60 90
ARCTAN δ
RELATIVE INTENSITY
45
40
35
30
25
J
0.608
1+
0.000
64Cu
J = 1
64Ni (p,n γ)64 Cu
Ep = 3.25 MeV
a2 = -0.360 ± 0.013
a4 = 0.011 ± 0.013
180 keV ABOVE THRESHOLD
J = 2
0.0
0.5
1.0
COS2 θ

Figure 8

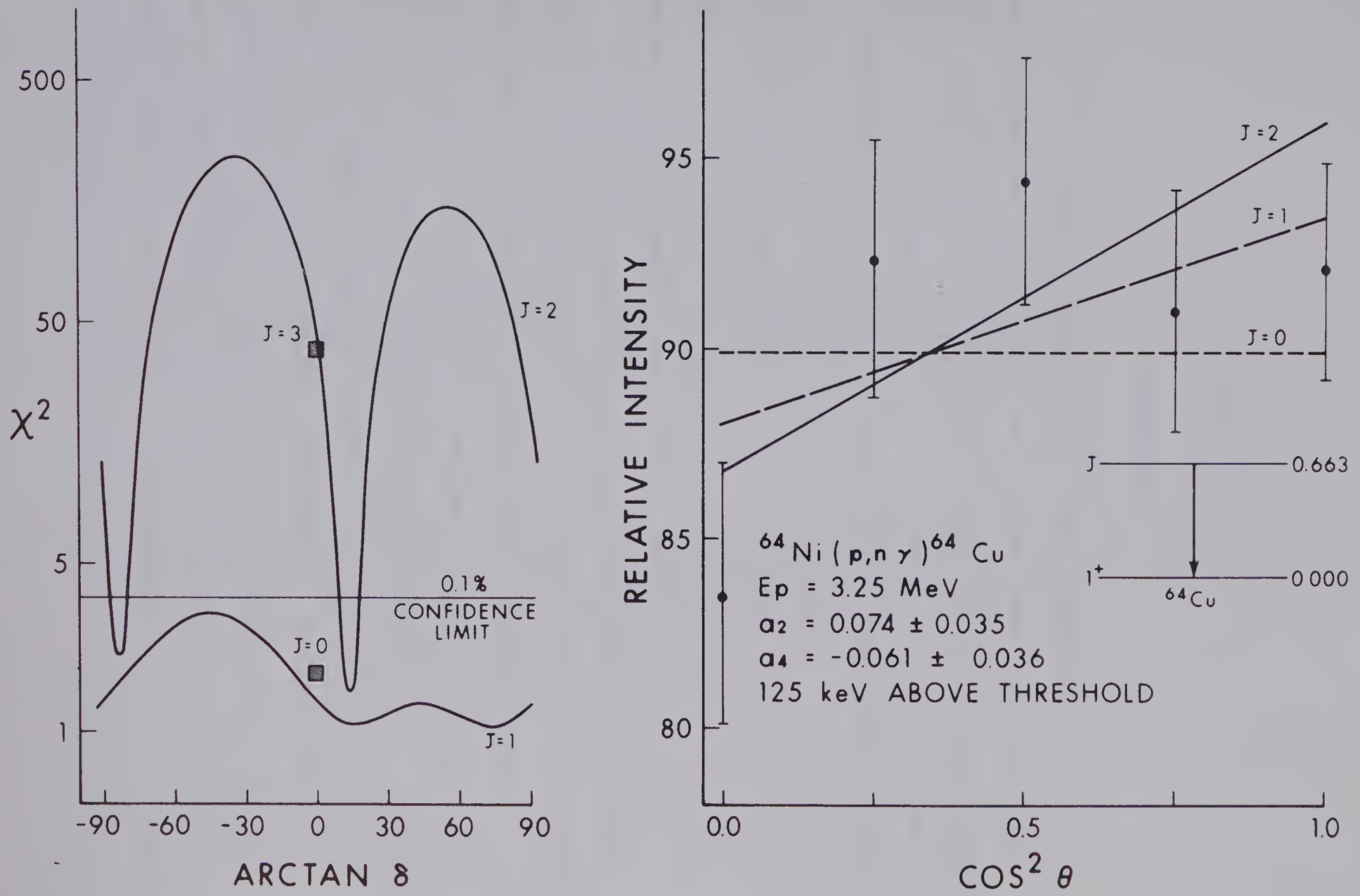
500
50
5
1
χ^2
J = 3
J = 2
J = 0
J = 1
0.1%
CONFIDENCE
LIMIT
-90 -60 -30 0 30 60 90
ARCTAN δ
RELATIVE INTENSITY
95
90
85
80
J = 2
J = 1
J = 0
^{64}Ni (p,n γ)^{64} Cu
Ep = 3.25 MeV
a_2 = 0.074 ± 0.035
a_4 = -0.061 ± 0.036
125 keV ABOVE THRESHOLD
J
0.663
1$^+$
0 000
^{64}Cu
0.0
0.5
1.0
COS^2 θ

Figure 9

CHAPTER 5

DISCUSSION

The main object of this study has been to determine some of the basic properties; such as spins, parities, and gamma-ray decay mixing and branching ratios, for the low-lying levels of ^{64}Cu. These quantities, however, are meaningless until they are compared to the predictions of a nuclear model. The validity of any particular model being the extent to which its predictions are confirmed by experiment. To date no model calculations have been carried out on the low-lying levels of ^{64}Cu and thus it is only possible to speculate as to the probable neutron and proton configurations and types of decay radiation that will occur.

For $^{64}_{29}Cu_{35}$ the low-lying states may be attributed to the various lowest seniority configurations that are possible for the eight nucleons, one proton and seven neutrons, lying outside the doubly-closed $1f^{7/2}$ shell. For low excitations these nucleons are assumed to occupy the $2p^{3/2}$, $1f^{5/2}$, and $2p^{1/2}$ orbitals; the proton occupying a $2p^{3/2}$ orbital, and the neutrons arranging themselves within these orbitals in such a manner as to form low seniority configurations. In fact, since the ground state of $^{63}_{29}Cu_{34}$ as pointed out by Thankappan and True (Th 64), can be attributed (85%) to the single uncoupled proton in the $2p^{3/2}$ orbital (the neutrons being zero coupled (seniority zero)), it is reasonable to suspect that the neutron configurations for ^{64}Cu will be of

seniority one. However, in order to obtain a realistic picture of these low excitation neutron configurations it is necessary to consider the ground state for $^{62}_{28}Ni_{34}$ and the low-lying states of $^{63}_{28}Ni_{35}$. From investigation of the $^{62}Ni(d,p)^{63}Ni$ reaction (Nu 67) the stripping cross sections to the ground state ($1/2^-$) and the first ($5/2^-$) and the second excited states ($3/2^-$) of ^{63}Ni have indicated ℓ_n transfers of 1, 3 and 1 respectively. These results indicate that the ^{63}Ni states probably contain neutron configurations of $(2p^{3/2})^2_0\ (1f^{5/2})^4_0\ (2p^{1/2})$, $(2p^{3/2})^2_0\ (1f^{5/2})^5_{5/2}$, and $(2p^{3/2})^3_{3/2}\ (1f^{5/2})^4_0$ respectively, which can be accounted for if ^{62}Ni has a ground state configuration containing $(2p^{3/2})^2_0\ (1f^{5/2})^4_0$. As these neutron states are energetically almost identical the low-lying states of ^{64}Cu may be considered by directly coupling a $2p^{3/2}$ proton to the neutron configurations representing the first three states of ^{63}Ni. The coupling of the $2p^{3/2}$ proton to the ground state neutron configuration $[(2p^{3/2})^2_0\ (1f^{5/2})^4_0\ (2p^{1/2})]$ results in the formation of states of spin 1^+ and 2^+. Similarly a $2p^{3/2}$ proton coupling to the $[(2p^{3/2})^2\ (1f^{5/2})^5_{5/2}]$ first excited state configuration results in the formation of states of spin 1^+, 2^+, 3^+ and 4^+ and coupling to the $[(2p^{3/2})^3_{3/2}(1f^{5/2})^4_0]$ configuration yields spin states of 0^+, 1^+, 2^+ and 3^+. In comparison with the level scheme of ^{64}Cu (figure 3) these configurations can be seen to account for the levels up to 700 keV excitation.

The γ-ray transitions between the states of such configurations must conserve angular momentum and parity. Consequently between states of configuration $[(2p^{3/2})]_p\ [(2p_0^{3/2})^2_0\ (1f^{5/2})^5_{5/2}]_n$ and those of $[(2p^{3/2})]_p$ $[(2p^{3/2})^2_0\ (1f^{5/2})^4_0\ (2p^{1/2})]_n$ and $[(2p^{3/2})]_p\ [(2p^{3/2})^3_{3/2}(1f^{5/2})^4_0]_n$ E2

transitions are to be expected; whereas for transitions between states of the same particle configuration, M1 transitions are expected. However if the states have configuration mixing, for example contributions from both the $[(2p^{3/2})]_p [(2p^{3/2})^2_0 (1f^{5/2})^5_{5/2}]_n$ and $[(2p^{3/2})]_p [(2p^{3/2})^2_0 (1f^{5/2})^4_0 (2p^{1/2})]_n$ configurations, then the transitions between these states will contian both M1 and E2 radiation. From the ^{63}Cu(d,p) investigation (Pa 69) the stripping cross sections for four states in ^{63}Cu below 500 keV excitation show contributions from ℓ_n = 1 and 3 transfers, thus indicating probable mixing of the particle configurations.

In order to obtain a more complete picture of this nucleus it would be advantageous to obtain lifetime measurements for the gamma transition.

REFERENCES

(Ba 53) G.A. Bartholomew and B.B. Kinsey, Phys. Rev. 89 (1953) 386

(Ba 64) G.A. Bartholomew and J. Vervier, Nucl. Phys. 50 (1964) 386

(BF 58) F. Bjorklund and S. Fernbach, Phys. Rev. 109 (1958) 1296

(Bl 52) J.W. Blatt and V.F. Weisskopf, Theoretical Nuclear Physics, 1952

(Co 62) B.L. Cohen, R.H. Fulmer and A.L. McCarthy, Phys. Rev. 126 (1962) 698

(Co 67) A.H. Colenbrander and T.J. Kennett, Can. J. Phys. 45 (1967) 2395

(Da 01) N.E. Davison, University of Alberta, Nuclear Research Centre internal report (1969) (unpublished)

(Da 70) W.F. Davidson, P.J. Dallimore and J. Hellstrom, Nucl. Phys. 142 (1970) 167

(Do 66) B.M. Dodsworth and H.A. Shugart, Phys. Rev. 142 (1966) 638

(Dr 01) M.M. Drum, University of Alberta, Privite communication.

(Dr 70) M.M. Drum, University of Alberta, Nuclear Research Centre internal report UAE-NPL-19 (1970) (unpublished)

(Du 68) F.E. Durham, S.G. Buccino and R.E. Rogan, Bull. Am. Phys. Soc. 13 (1968) 725

(Er 63) T. Ericson, Annals of Physics 23 (1963) 390

(Fi 58) R.P. de Figueiredo, M. Mazari and W.W. Buechner, Phys. Rev. 112 (1958) 873

(Gr 70) P.W. Green and M.M. Drum, University of Alberta, Nuclear Research Centre internal report (1970) (unpublished)

(Gu 68) D.P. Gurd, Ph. D. Thesis, University of Alberta (1967) (unpublished)

(Ha 52) W. Hauser and H. Feshbach, Phys. Rev. 87 (1952) 366

(Hj 66) S.A. Hjorth and L.H. Allen, Ark. Fys. 33 (1967) 207

(Ko 65) J. Kopecky, J. Kajfosz and B. Chalupa, Nucl. Phys. 68 (1965) 449

(Ko 69) J. Kopecky and E. Warming, Nucl. Phys. 127 (1969) 385

(Le 54) A. Lemonick and F.M. Pipkin, Phys. Rev. 95 (1954) 1356

(Li 64) A.E. Litherland, Radiative Transitions following Nuclear Reactions, Scottish Universities Summer School in Physics, Edinburgh (1964) 3

(Lo 51) S.P. Lloyd, Phys. Rev. 81 (1951) 161

(Nu 64) Nuclear Reaction Q-Values, University of California (1964) UCRL-16964

(Nu 67) Nuclear Data, B2-3-33 (1967)

(OB 67) P.J. O'Brien, Nucl. Phys. 104 (1967) 609

(Pa 69) Y.S. Park and W.W. Daehnick, Phys. Rev. 180 (1969) 1082

(PB 62) F.G. Perey and B. Buck, Nucl. Phys. 32 (1962) 353

(Pe 63) F.G. Perey, Phys. Rev. 131 (1963) 745

(Ro 66) L. Rosen, Proc. 2nd Int. Symp. on Polarization Phenomena of Nucleons, Karlsruhe, Sept. 1965, ed. P. Huber and H. Schopper, (Birkhauser Verlag, Basel (1966) 253)

(Ro 67) H.J. Rose and D.M. Brink, Rev. Mod. Phys. 39 (1967) 306

(Sh 66) E. Sheldon and D.M. van Patter, Rev. Mod. Phys. 38 (1966) 143

(Sh 68) E.B. Shera and H.H. Bolotin, Phys. Rev. 169 (1968) 940

(Sh 69) E. Sheldon and R.M. Strang, Computer Phys. Com. 1 (1969) 35

(Te 66) J.W. Tepel, Nucl. Inst. Meth. 40 (1966) 100

(Th 64) V.K. Thankappan and W.W. True, Phys. Rev. 137(1965) 793

(To 61) S.J. Du Toit and L.M. Bollinger, Phys. Rev. 123 (1961) 449

(Tr 57) G. Trumpy, Nucl. Phys 2 (1957) 664

(Ve 61) J. Vervier, Nucl. Phys. 26 (1961) 10

(Vo 68) E. Vogt, Advances in Nuclear Physics (Plenum Press, New York,(1968) 261)

(We 69) C.C. Wellborn and S.G. Buccino, Tulane University (1969) (unpublished)

(Yo 68) H.J. Young, Bull. Am. Phys. Soc. 13 (1968) 105

APPENDIX

THE DEPENDANCE OF THE a_K COEFFICIENTS, PREDICTED BY THE COMPOUND NUCLEAR STATISTICAL MODEL, ON THE ENERGY-DEPENDANT TRANSMISSION COEFFICIENTS

APPENDIX

The angular distribution of a gamma-ray decaying between states of definite parity can be expressed in the form

$$W(\theta) = \sum_{K \text{ even}} a_K P_K(\cos\theta)$$

For a (p,nγ) reaction the a_K expansion coefficients can be expressed in terms of Clebsch-Gordan and Racah coefficients, the multipole mixing ratio, and the transmission coefficients of the penetrability term τ (equation 12). As the population parameters of the initial state (the residual state in the (p,n) reaction) are expressed directly in terms of the partial wave proton and neutron transmission coefficients the anisotropy of the gamma-ray angular distribution becomes extremely sensitive to the relative magnitudes of these quantities, in particular to the ratio $T_{\ell_n=\ell'}(E_n)/T_{\ell_n=0}(E_n)$, ℓ' being the order of neutron partial wave. Figure 1 shows plots of the ratios of $T_{\ell_n=1}(E_n)/T_{\ell_n=0}(E_n)$ and $T_{\ell_n=2}/T_{\ell_n=0}$ as a function of energy above threshold for the ^{64}Ni(p,nγ) ^{64}Cu reaction.

For proton energies close to the neutron threshold i.e. $E_n < 200$ keV, the higher order neutron partial waves are small, and the penetrability term becomes dependent only on the relative magnitude of the s and p partial wave neutron transmission coefficients. This is essentially what

keeps the residual nucleus aligned as there is no opportunity for the higher magnetic states to become populated. However as the energy of the neutrons decaying from the compound nucleus increases the contribution of the higher order partial waves in penetrability then become appreciable. Under such conditions the residual state in the (p,n) reaction (i.e. the initial gamma-ray state) will only be weakly aligned.

The predicted a_2 and a_4 coefficients for all possible spin sequences and mixing ratios occurring for a gamma-day decay to states of spin 1^+, 2^+, 3^+ and 4^+ have been calculated for proton energies of 50 keV, 150 keV, 300 keV, and 500 keV above threshold (figures 4a to 7b). Although these a_K contour plots have been calculated for the specific case of the $^{64}Ni(p,n\gamma)^{64}Cu$ reaction in general they are applicable for any $(p,n\gamma)$ reaction on medium weight, spin 0^+, target nuclei.

The transmission coefficients were calculated using the programme Hauser (Da 01). As a means of checking the sensitivity of the transmission coefficients, and thus the predicted a_K coefficients, to the optical model parameters four different sets of transmission coefficients were obtained. The a_K predictions for all possible spin sequences and multipole mixing ratios for a gamma-ray decay to states of spin 1^+ and 2^+ at a proton energy 100 keV above threshold were obtained for each set of neutron transmission coefficients. These results are shown in figures 2a to 3d.

Figure 1 Plots of the ratio of the neutron transmission coefficients $T_{\ell=1}/T_{\ell=0}$ and $T_{\ell=2}/T_{\ell=0}$ as a function of outgoing energy. The transmission coefficients were calculated using the computer code Hauser (Da 01) and the neutron optical model parameters of Perey (Pe 63).

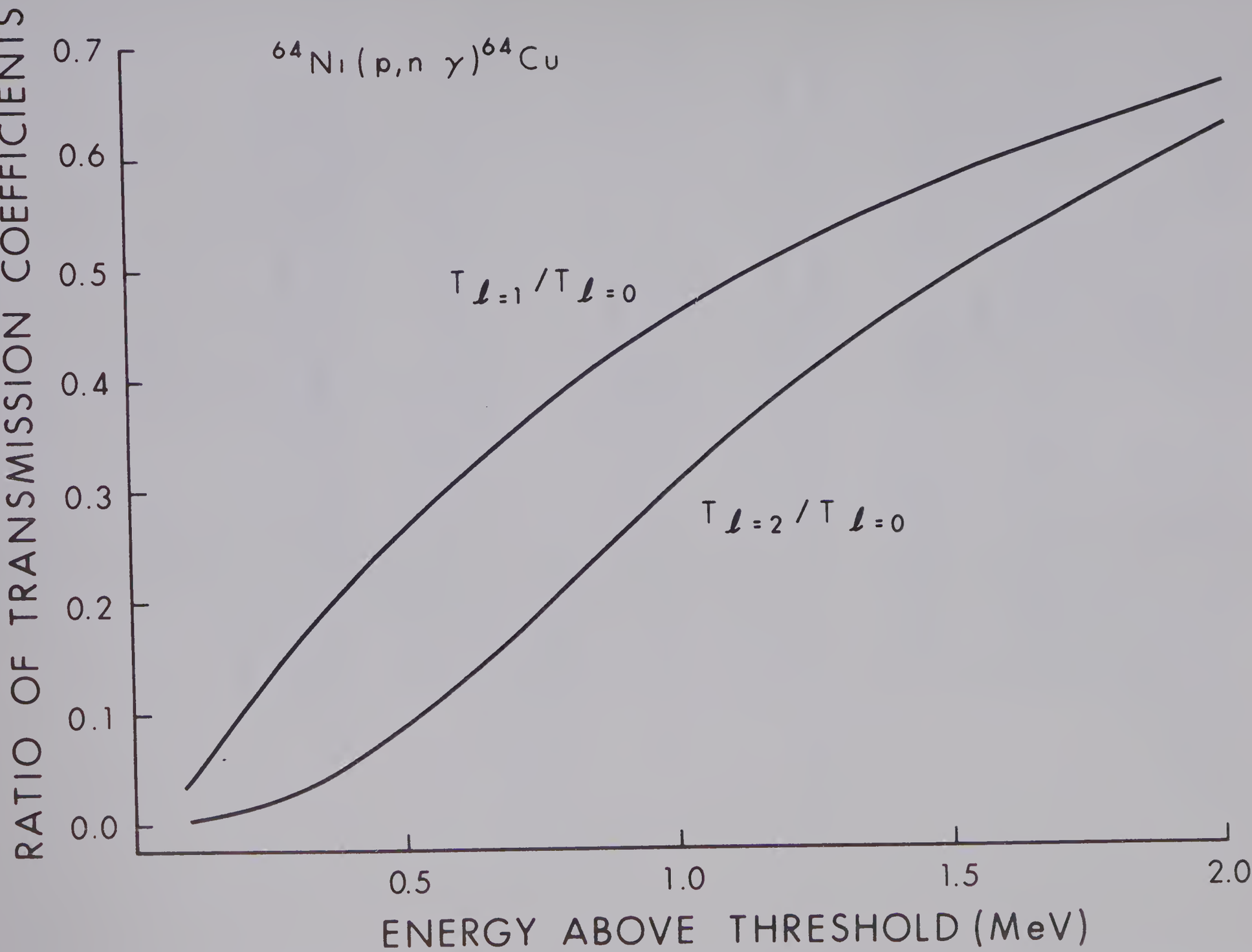
$^{64}Ni(p,n\gamma)^{64}Cu$
$T_{\ell=1}/T_{\ell=0}$
$T_{\ell=2}/T_{\ell=0}$
RATIO OF TRANSMISSION COEFFICIENTS
0.0
0.1
0.2
0.3
0.4
0.5
0.6
0.7
0.5
1.0
1.5
2.0
ENERGY ABOVE THRESHOLD (MeV)

Figure 1

Plots of the a_2 and a_4 multipole ellipses as predicted by the compound nuclear statistical model from four different sets of neutron transmission coefficients for a gamma-ray decay to a state of spin 1^+ in ^{64}Cu at an incident energy 100 keV above threshold.

Figure 2a) Transmission coefficients were determined for the computer code Hauser (Da 01) and the neutron optical model parameters of Perey (Pe 63).

2b) Transmission coefficients were determined from the computer code Hauser and the neutron optical model parameters of Rosen (Ro 67).

2c) Transmission coefficients were determined from the computer code Hauser and the neutron optical model parameters of Bjorklund-Fernbach (BF 58).

2d) Transmission coefficients were determined from the computer code Hauser and the neutron optical model parameters of Perey-Buck (PB 62).

NEUTRON OPTICAL MODEL PARAMETERS

V_o = 48.0 MeV W_o = 9.6 MeV

r_r = 1.27 fm r_i = 1.25 fm

a_r = 0.66 fm a_i = 0.47 fm

V_{so} = 7.2 MeV

Ep = 100 keV ABOVE THRESHOLD

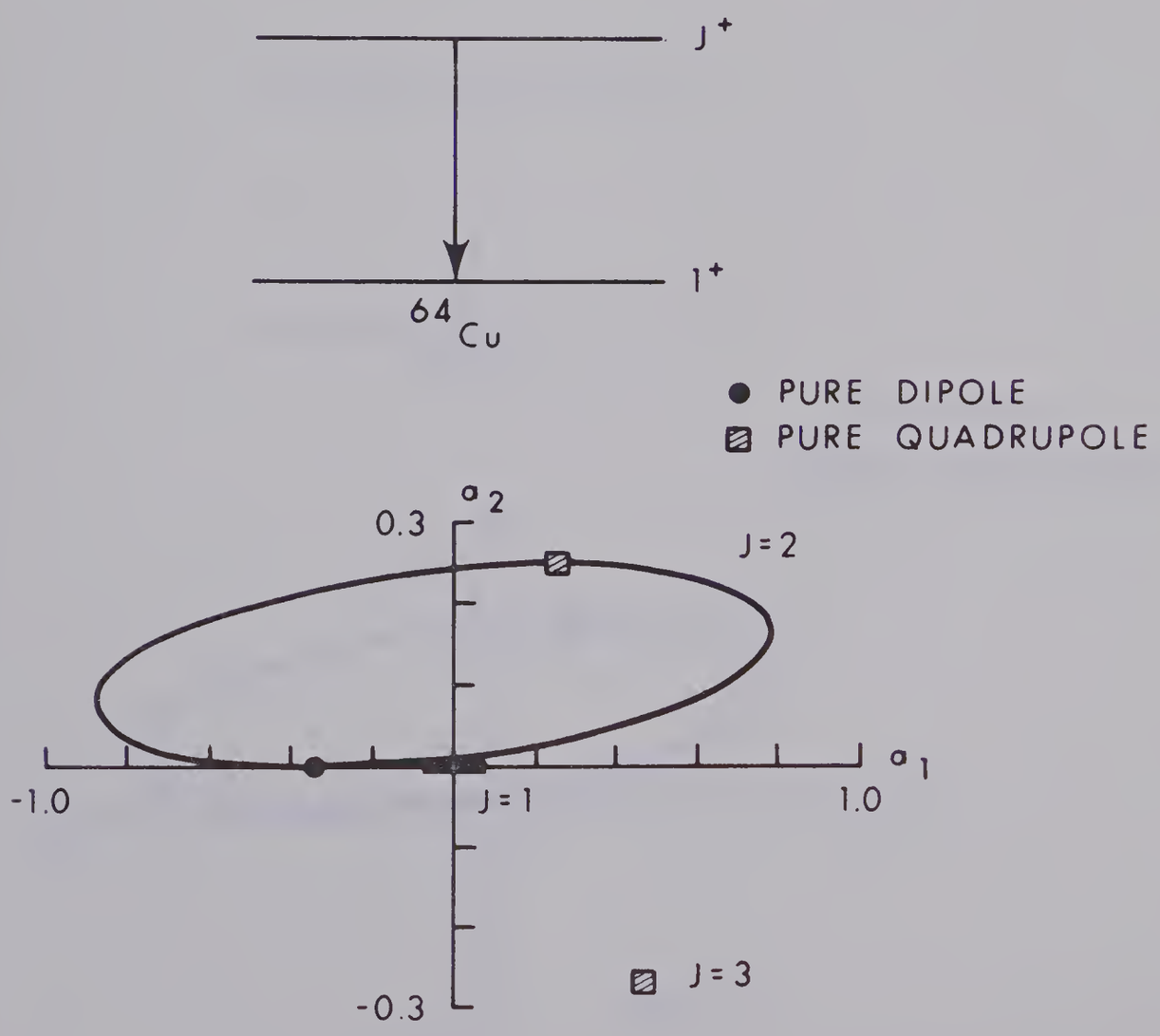

Figure 2a

NEUTRON OPTICAL MODEL PARAMETERS

V_o = 49.5 MeV W_o = 5.75 MeV

r_r = 1.25 fm r_i = 1.25 fm

a_r = 0.65 fm a_i = 0.70 fm

V_{so} = 5.5 MeV

Ep = 100 keV ABOVE THRESHOLD

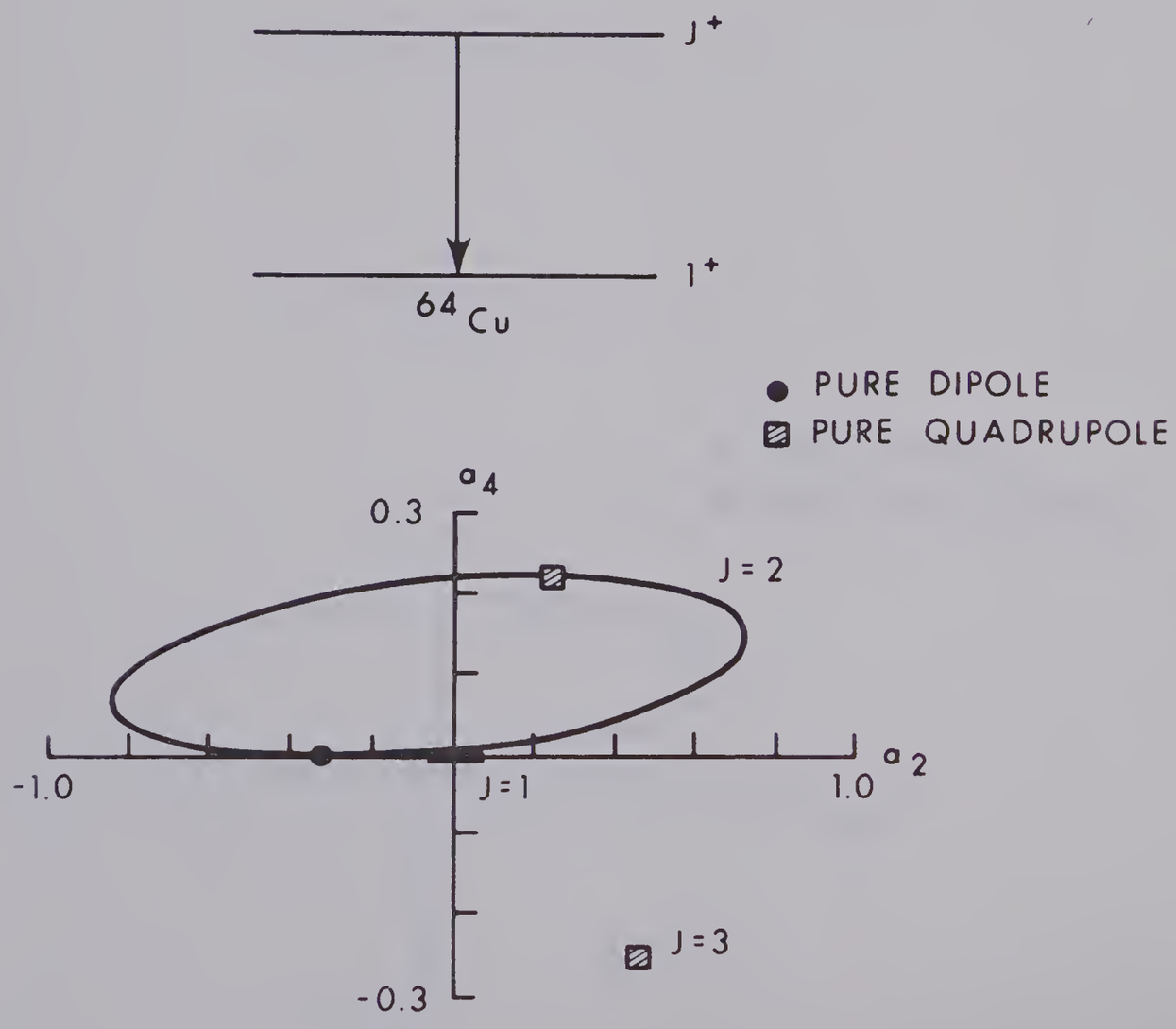

Figure 2b

NEUTRON OPTICAL MODEL PARAMETERS

V_o = 50.0 MeV W_o = 7.0 MeV

r_r = 1.25 fm r_i = 1.25 fm

a_r = 0.65 fm a_i = 0.98 fm

V_{so} = 9.5 MeV

Ep = 100 keV ABOVE THRESHOLD

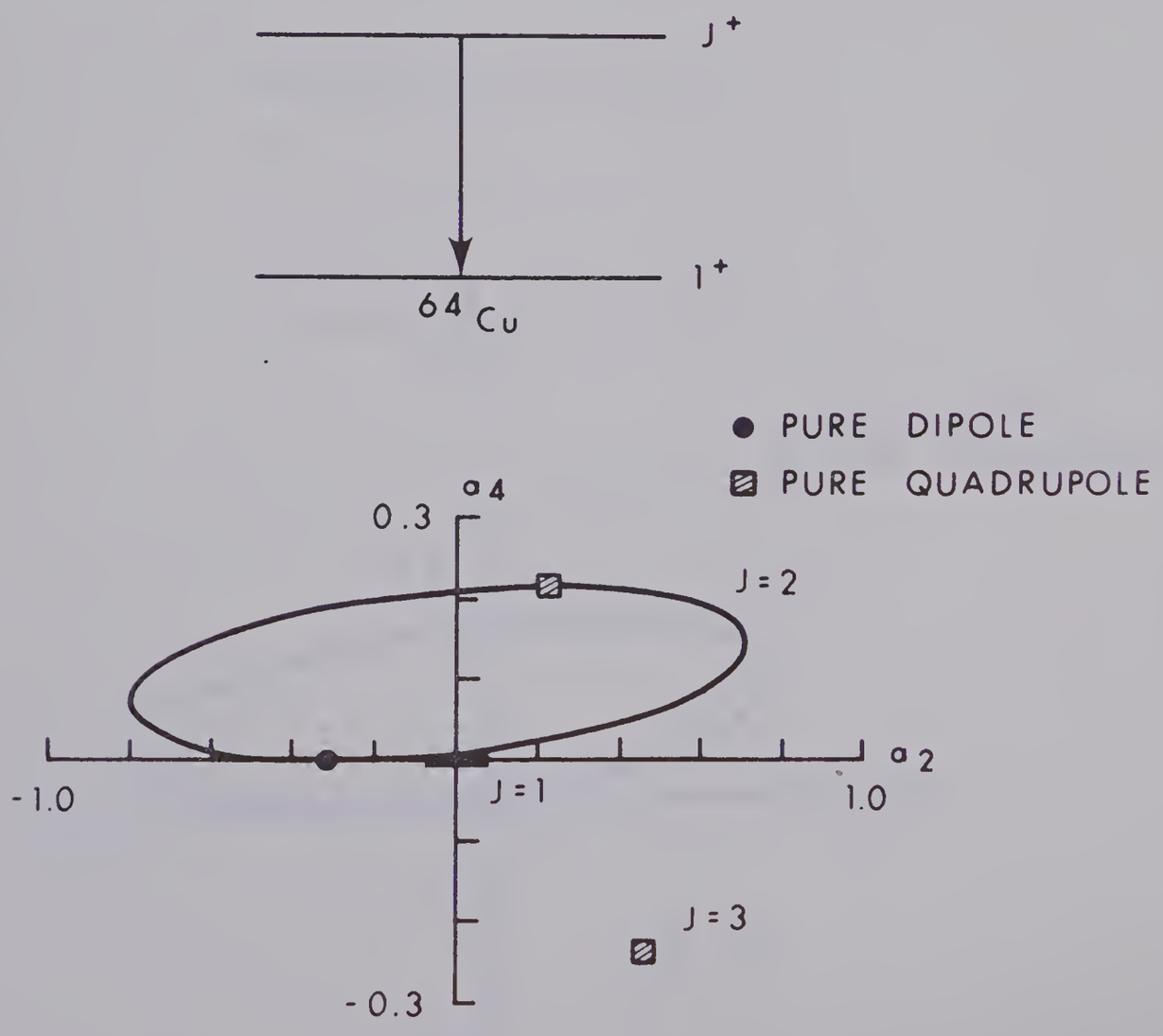

Figure 2c

NEUTRON OPTICAL MODEL PARAMETERS

V_o = 41.35 MeV W_o = 3.95 MeV

r_r = 1.32 fm r_i = 1.32 fm

a_r = 0.62 fm a_i = 0.65 fm

V_{so} = 7.2 MeV

Ep = 100 keV ABOVE THRESHOLD

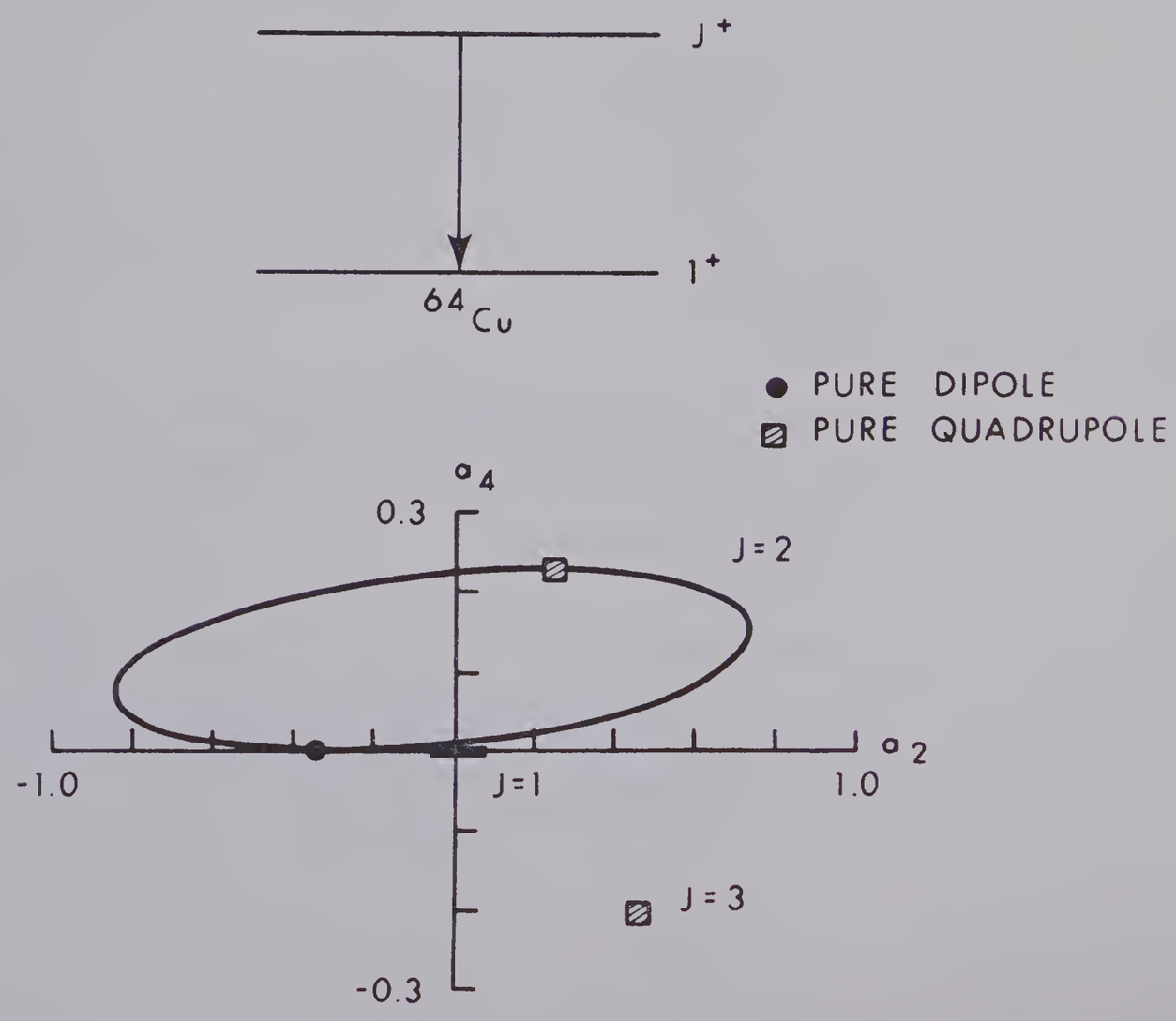

Figure 2d

Plots of the a_2 and a_4 multipole ellipses as predicted by the compound nuclear statistical model from four different sets of neutron transmission coefficients for a gamma-ray decay to a state of spin 2^+ in ^{64}Cu at an incident energy 100 keV above threshold.

Figure 3a) Transmission coefficients were determined from the computer code Hauser (Da 01) and the neutron optical model parameters of Perey (Pe 63).

3b) Transmission coefficients were determined from the computer code Hauser and the neutron optical model parameters of Rosen (Ro 67)

3c) Transmission coefficients were determined from the computer code Hauser and the neutron optical model parameters of Bjorklund-Fernbach (BF 58).

3d) Transmission coefficients were determined from the computer code Hauser and the neutron optical model parameters of Perey-Buck (PB 62).

NEUTRON OPTICAL MODEL PARAMETERS

V_o = 48.0 MeV W_o = 9.6 MeV

r_r = 1.27 fm r_i = 1.25 fm

a_r = 0.66 fm a_i = 0.47 fm

V_{so} = 7.2 MeV

Ep = 100 keV ABOVE THRESHOLD

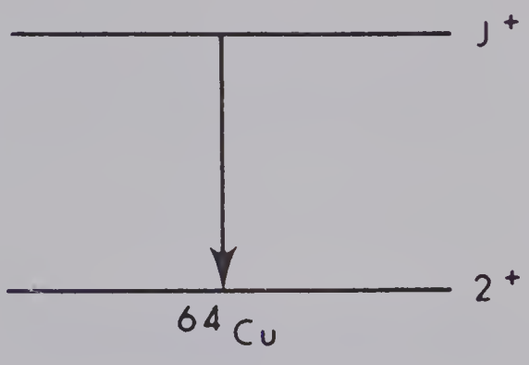

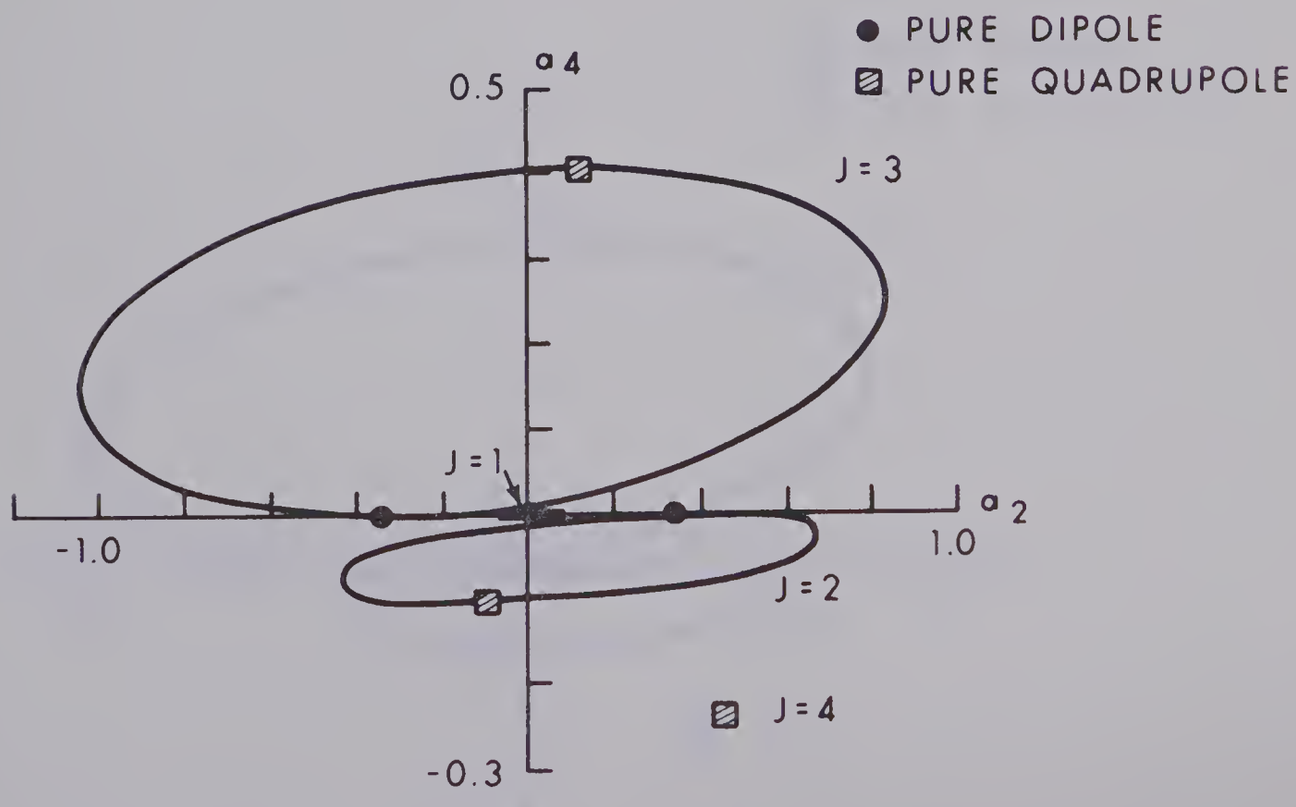

Figure 3a

NEUTRON OPTICAL MODEL PARAMETERS

V_o = 49.5 MeV W_o = 5.75 MeV

r_r = 1.25 fm r_i = 1.25 fm

a_r = 0.65 fm a_i = 0.70 fm

V_{so} = 5.5 MeV

Ep = 100 keV ABOVE THRESHOLD

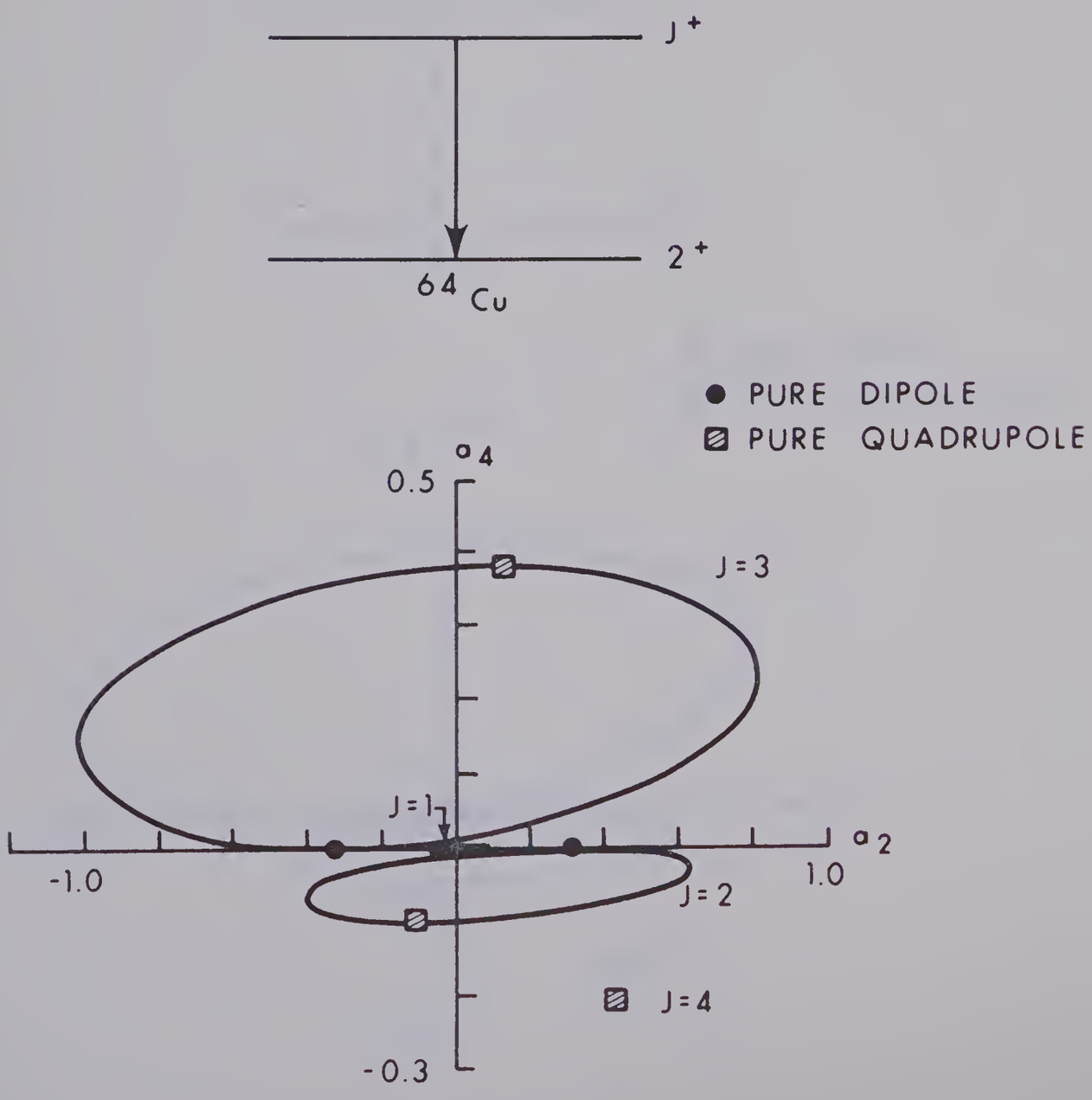

Figure 3b

NEUTRON OPTICAL MODEL PARAMETERS

V_o = 50.0 MeV W_o = 7.0 MeV

r_r = 1.25 fm r_i = 1.25 fm

a_r = 0.65 fm a_i = 0.98 fm

V_{so} = 9.5 MeV

Ep = 100 keV ABOVE THRESHOLD

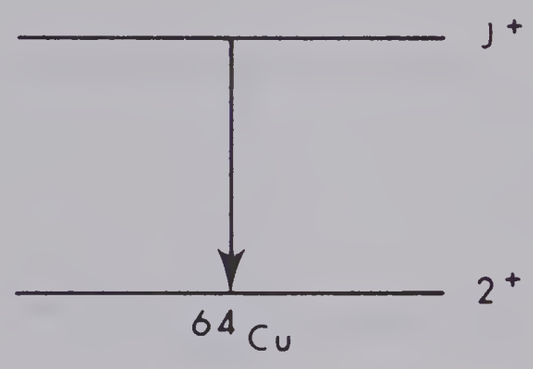

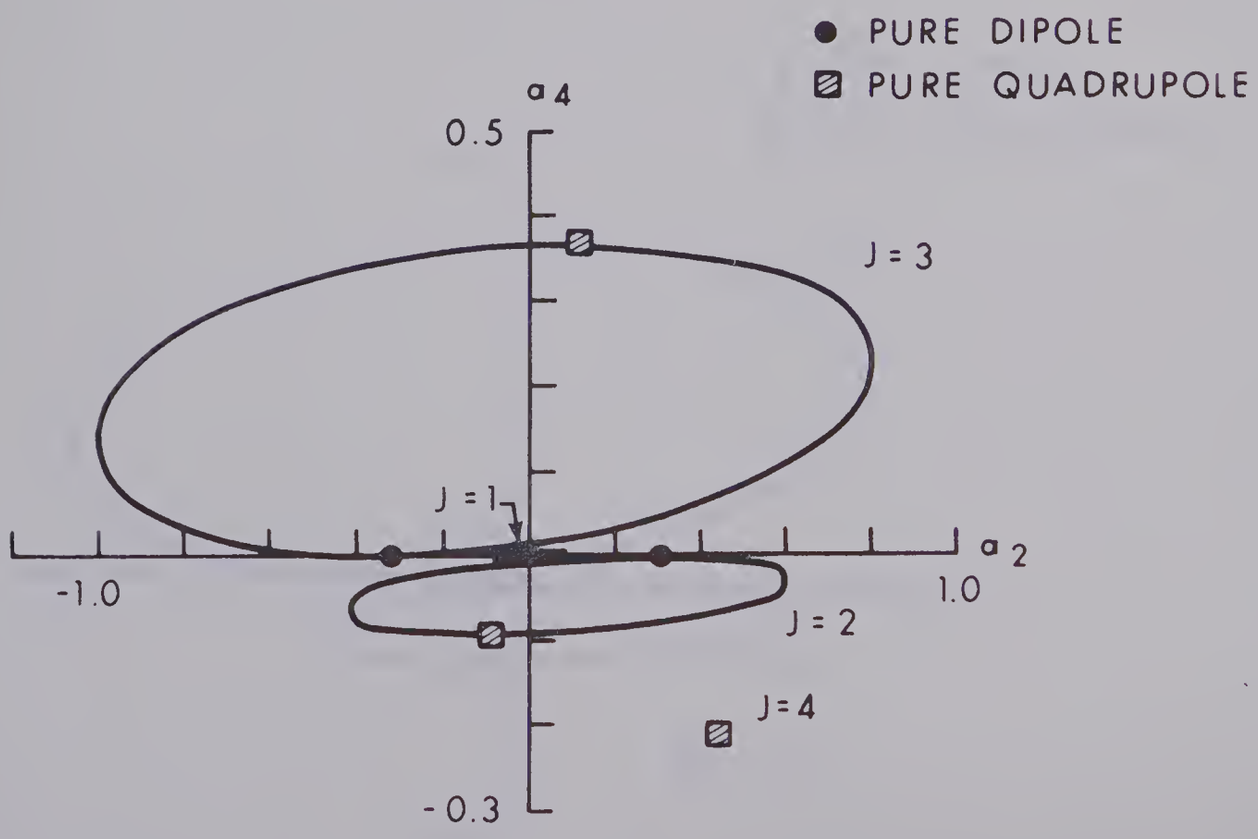

Figure 3c

NEUTRON OPTICAL MODEL PARAMETERS

V_o = 41.35 MeV W_o = 3.95 MeV

r_r = 1.32 fm r_i = 1.32 fm

a_r = 0.62 fm a_i = 0.65 fm

V_{so} = 7.2 MeV

Ep = 100 keV ABOVE THRESHOLD

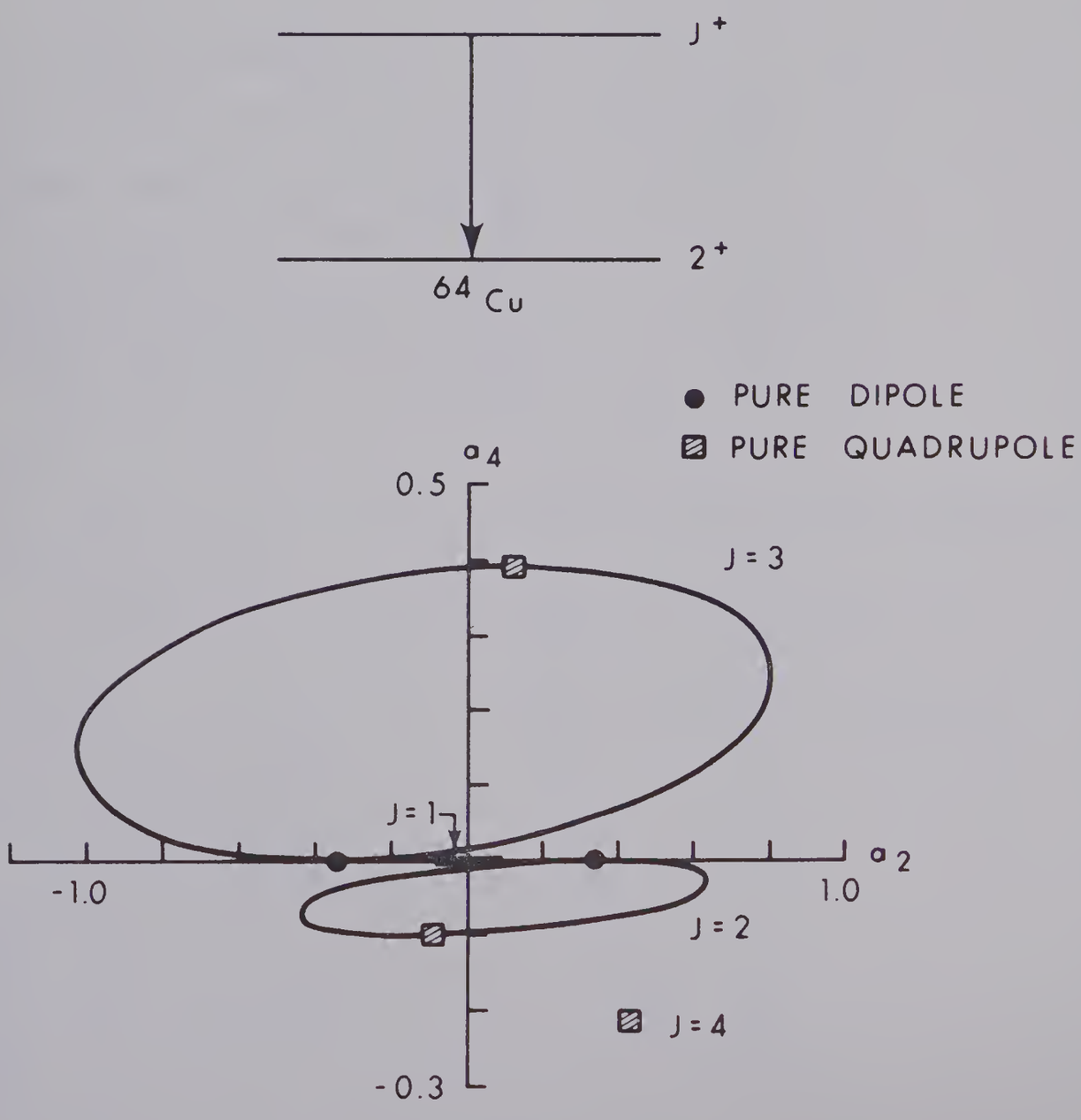

Figure 3d

Plots of the a_2 and a_4 multipole ellipses as predicted by the compound nuclear statistical model for a gamma ray decay to a state of spin 1^+ in ^{64}Cu for incident energies 50 keV, 150 keV, 300 keV, and 500 keV above threshold. Transmission coefficients were determined from the computer code Hauser (Da 01) and the neutron optical model parameters of Perey (Pe 63).

Figure 4a) Proton energies 50 keV and 150 keV above threshold.

4b) Proton energies 300 keV and 500 keV above threshold.

NEUTRON OPTICAL MODEL PARAMETERS

V_o = 48.0 MeV W_o = 9.6 MeV

r_r = 1.27 fm r_i = 1.25 fm

a_r = 0.66 fm a_i = 0.47 fm

V_{so} = 7.2 MeV

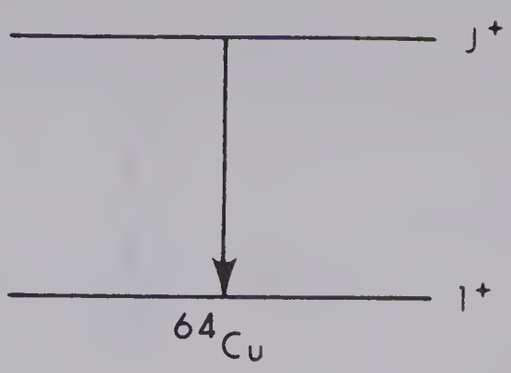

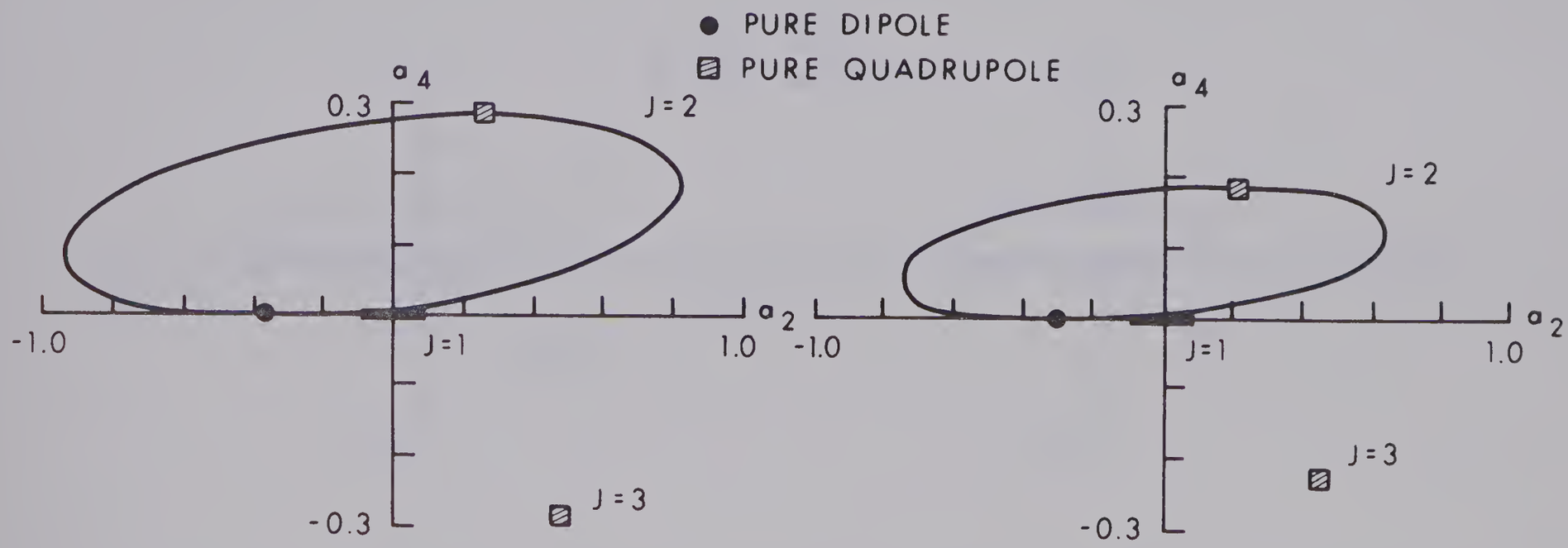

Ep= 50 keV ABOVE THRESHOLD Ep =150 keV ABOVE THRESHOLD

Figure 4a

NEUTRON OPTICAL MODEL PARAMETERS

V_o = 48.0 MeV W_o = 9.6 MeV

r_r = 1.27 fm. r_i = 1.25 fm

a_r = 0.66 fm a_i = 0.47 fm

V_{so} = 7.2 MeV

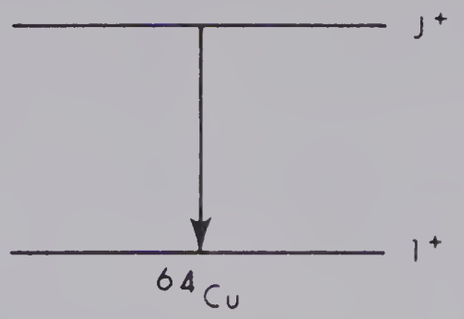

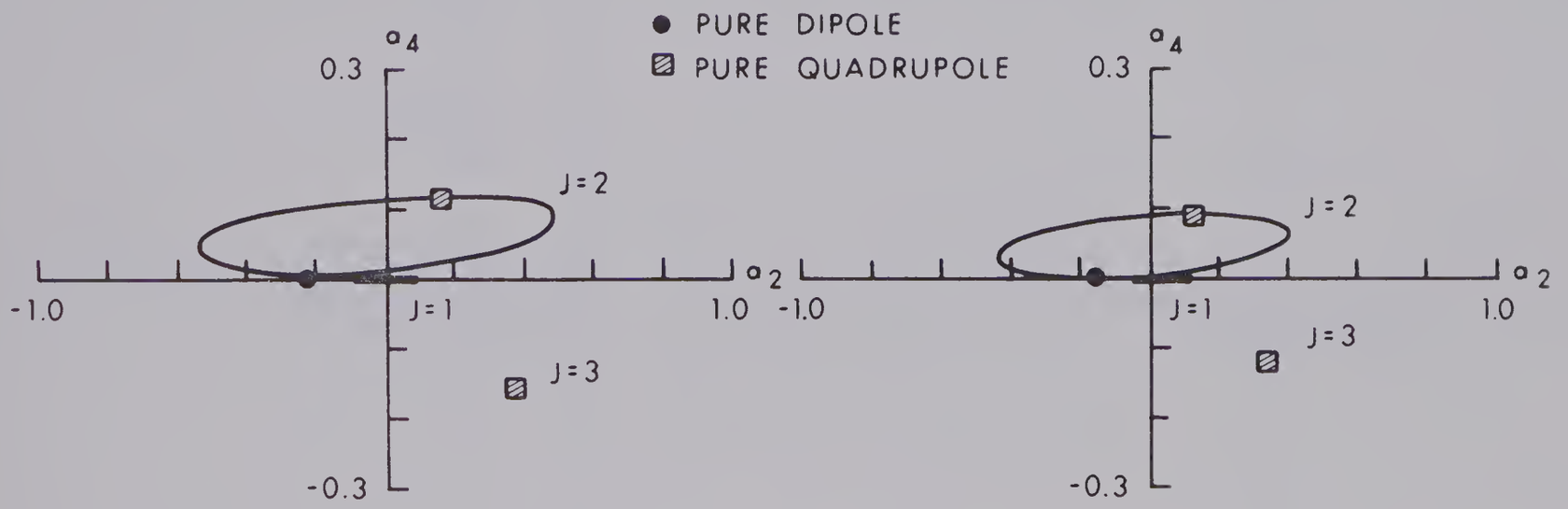

Ep = 300 keV ABOVE THRESHOLD Ep = 500 keV ABOVE THRESHOLD

Figure 4b

Plots of the a_2 and a_4 multipole ellipses as predicted by the compound nuclear statistical model for a gamma ray decay to a state of spin 2^+ in ^{64}Cu for incident energies 50 keV, 150 keV, 300 keV, and 500 keV above threshold. Transmission coefficients were determined from the computer code Hauser (Da 01) and the neutron optical model parameters of Perey (Pe 63).

Figure 5a) Proton energies 50 keV and 150 keV above threshold.

5b) Proton energies 300 keV and 500 keV above threshold.

NEUTRON OPTICAL MODEL PARAMETERS

V_o = 48.0 MeV W_o = 9.6 MeV

r_r = 1.27 fm r_i = 1.25 fm

a_r = 0.66 fm a_i = 0.47 fm

V_{so} = 7.2 MeV

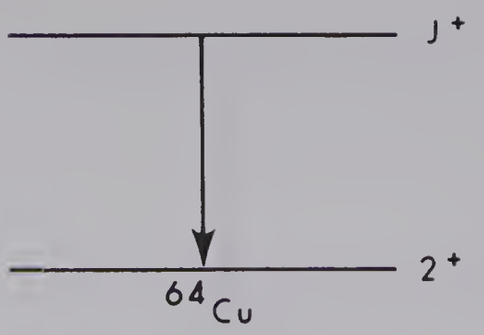

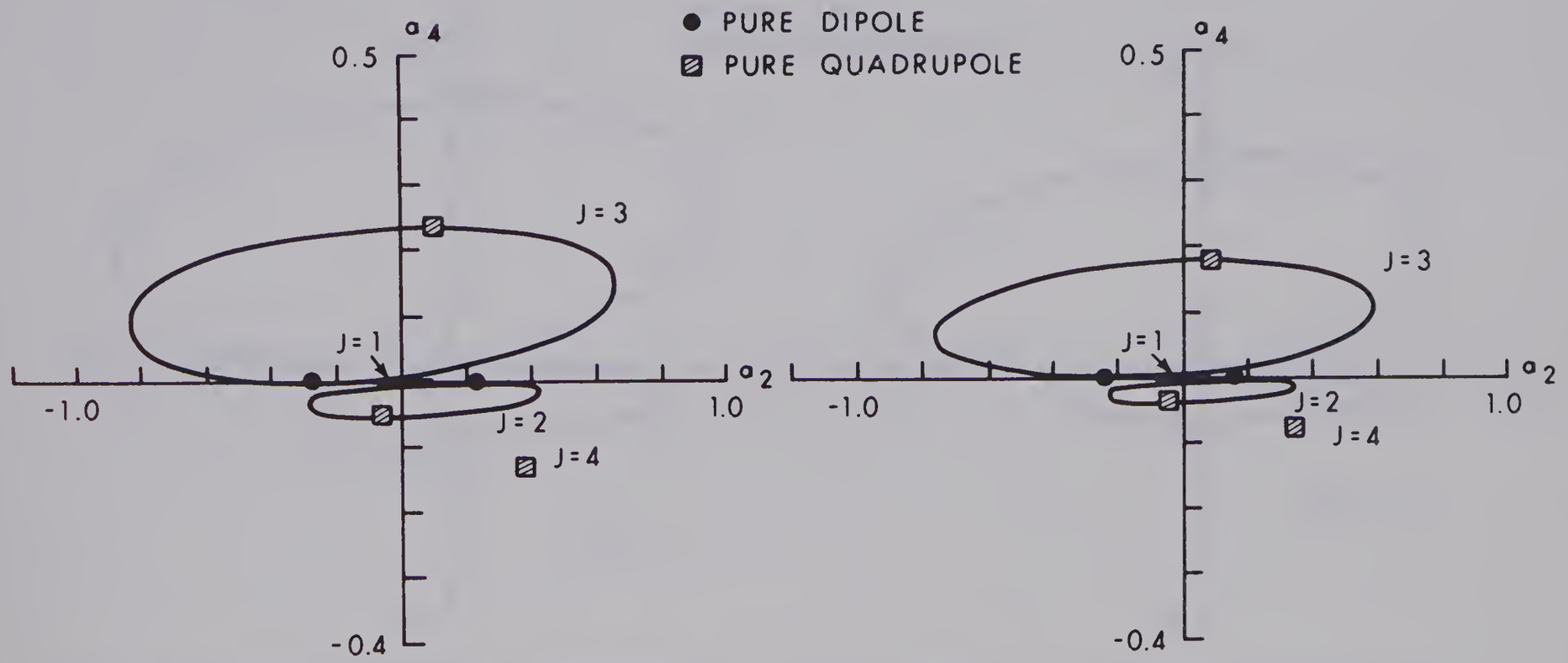

Ep = 300 keV ABOVE THRESHOLD Ep = 500 keV ABOVE THRESHOLD

Figure 5a

NEUTRON OPTICAL MODEL PARAMETERS

V_o = 48.0 MeV W_o = 9.6 MeV

r_r = 1.27 fm r_i = 1.25 fm

a_r = 0.66 fm a_i = 0.47 fm

V_{so} = 7.2 MeV

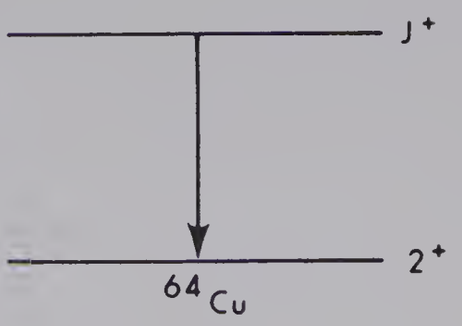

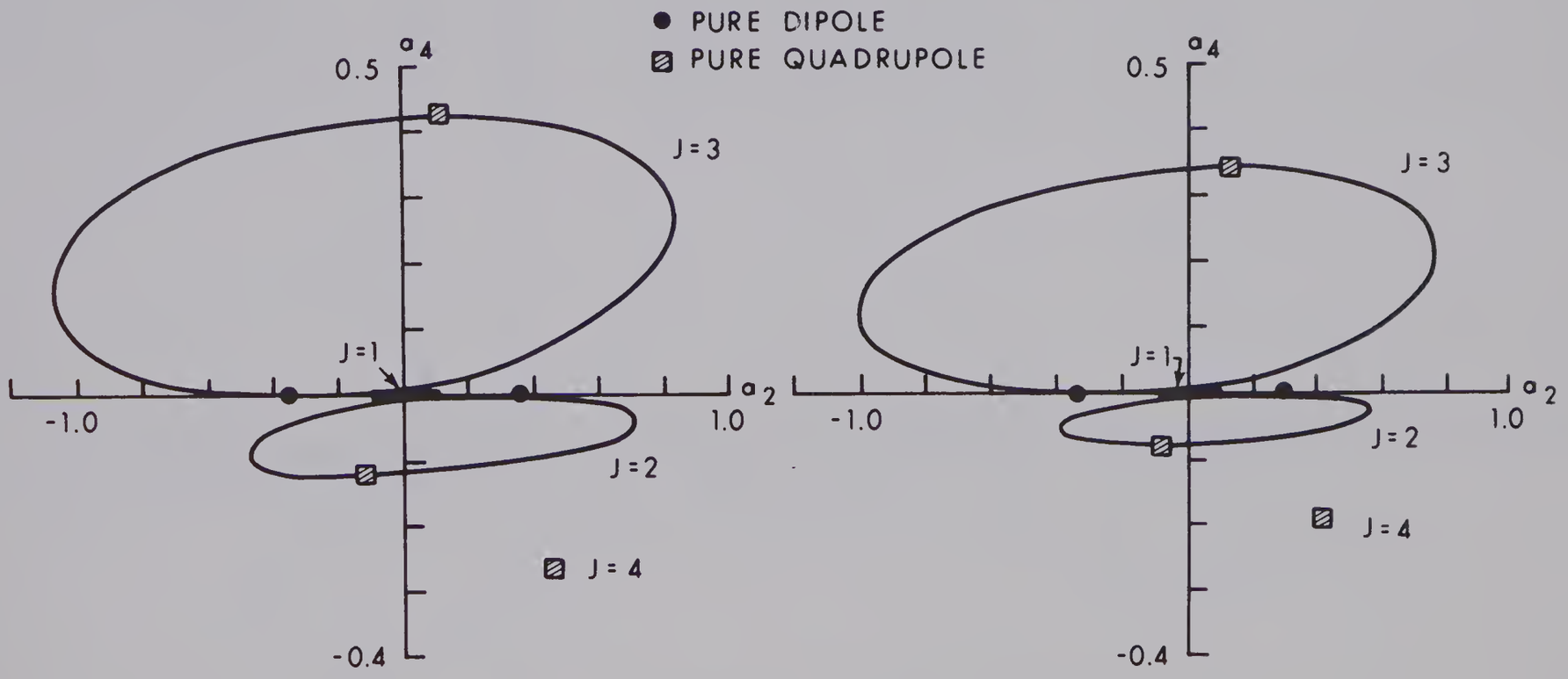

Ep = 50 keV ABOVE THRESHOLD Ep = 150 keV ABOVE THRESHOLD

Figure 5b

Plots of the a_2 and a_4 multipole ellipses as predicted by the compound nuclear statistical model for a gamma ray decay to a state of spin 3^+ in ^{64}Cu for incident energies 50 keV, 150 keV, 300 keV and 500 keV above threshold. Transmission coefficients were determined from the computer code Hauser (Da 01) and the neutron optical model parameters of Perey (Pe 63).

Figure 6a) Proton energies 50 keV and 150 keV above threshold.

6b) Proton energies 300 keV and 500 keV above threshold.

NEUTRON OPTICAL MODEL PARAMETERS

V_o = 48.0 MeV W_o = 9.6 MeV

r_r = 1.27 fm r_i = 1.25 fm

a_r = 0.66 fm a_i = 0.47 fm

V_{so} = 7.2 MeV

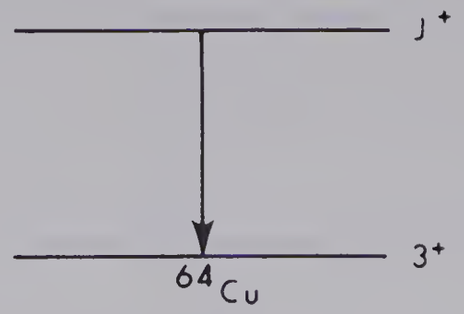

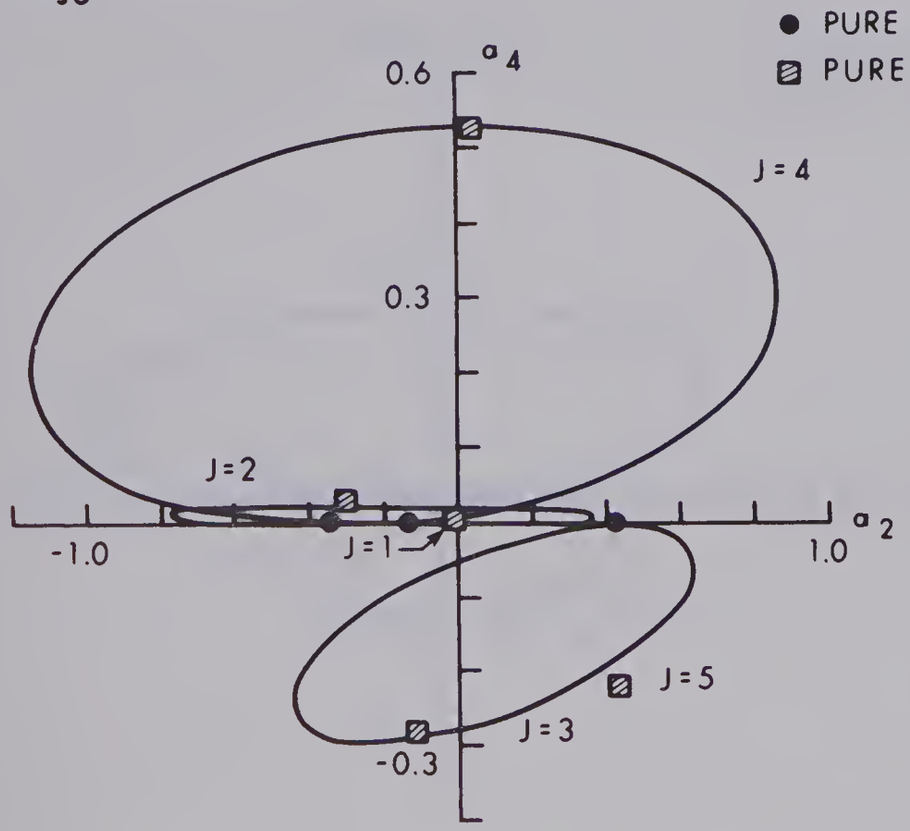

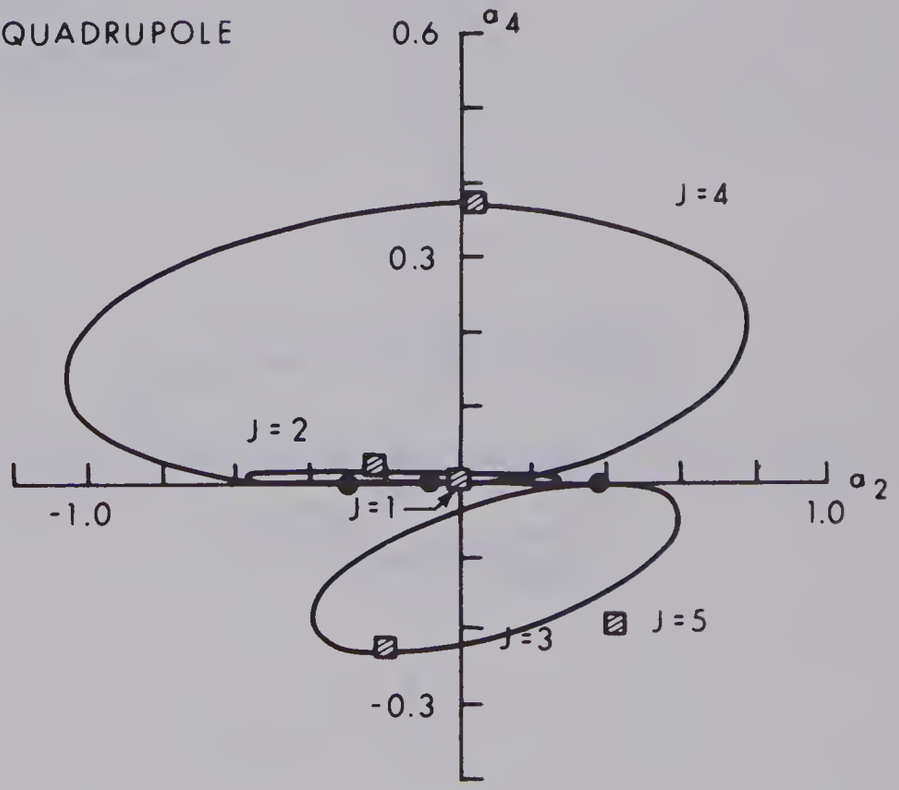

Ep = 50 keV ABOVE THRESHOLD

Ep = 150 keV ABOVE THRESHOLD

Figure 6a

NEUTRON OPTICAL MODEL PARAMETERS

V_o = 48.0 MeV W_o = 9.6 MeV

r_r = 1.27 fm r_i = 1.25 fm

a_r = 0.66 fm a_i = 0.47 fm

V_{so} = 7.2 MeV

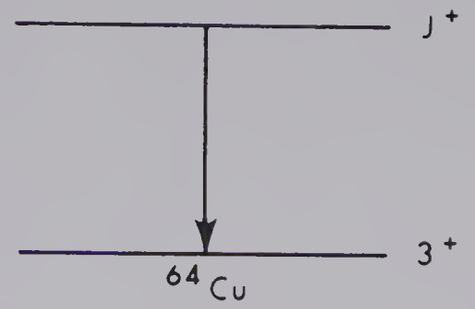

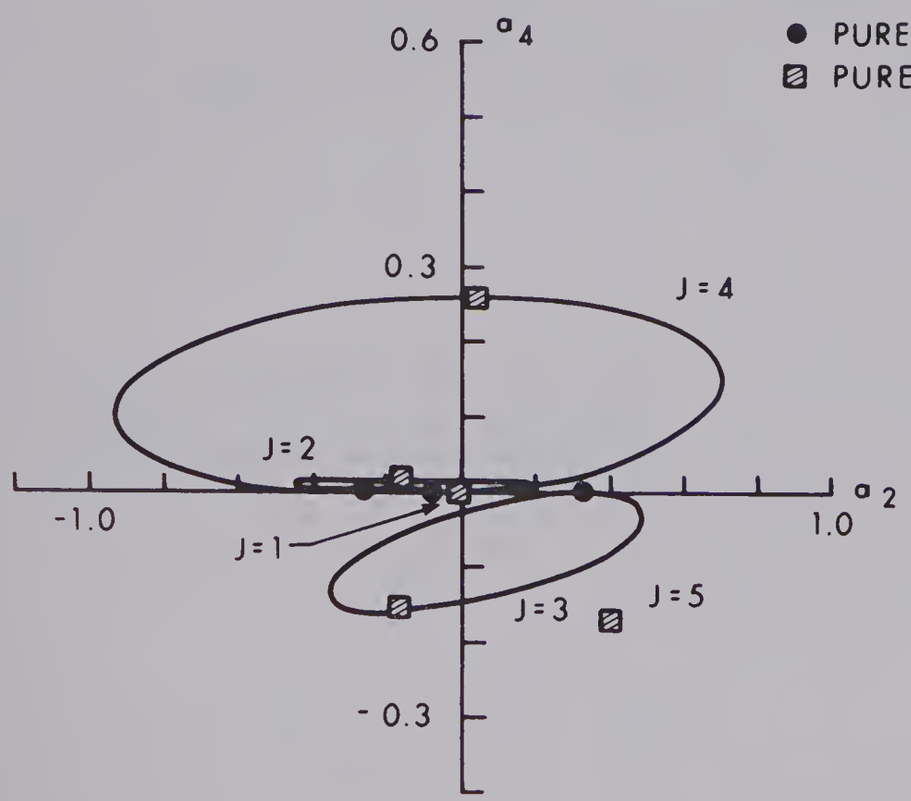

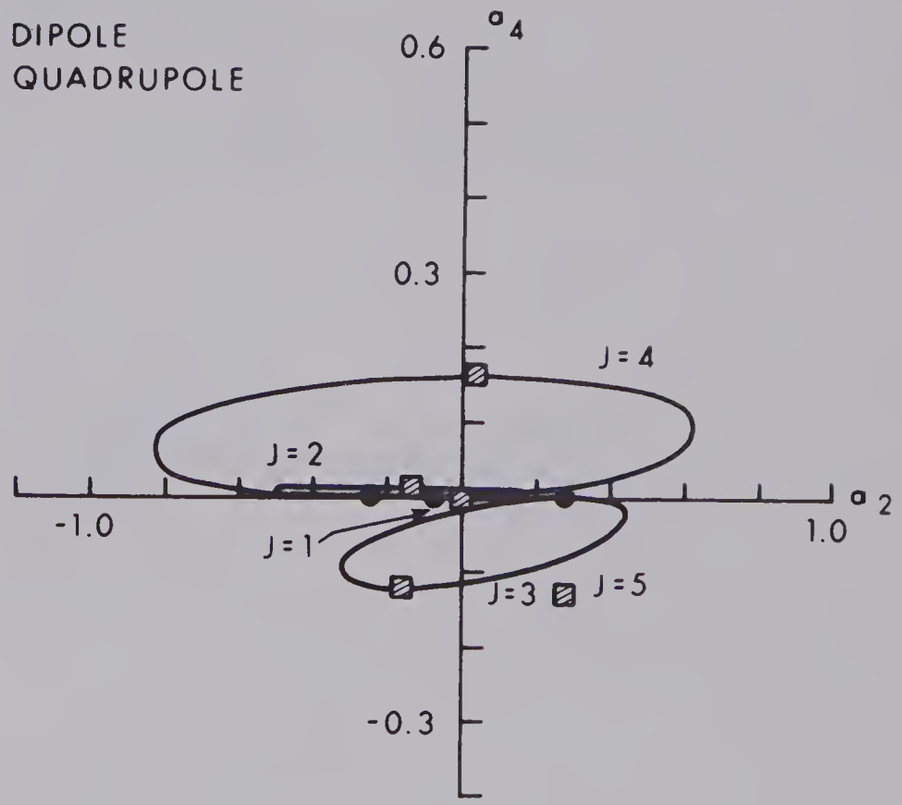

Ep = 300 keV ABOVE THRESHOLD

Ep = 500 keV ABOVE THRESHOLD

Figure 6b

Plots of the a_2 and a_4 multipole ellipses as predicted by the compound nuclear statistical model for a gamma ray decay to a state of spin 4^+ in ^{64}Cu for incident energies 50 keV, 150 keV, 300 keV, and 500 keV above threshold. Transmission coefficients were determined from the computer code Hauser (Da 01) and the neutron optical model parameters of Perey (Pe 63).

Figure 7a) Proton energies 50 keV and 150 keV above threshold.

7b) Proton energies 300 keV and 500 keV above threshold.

NEUTRON OPTICAL MODEL PARAMETERS

V_o = 48.0 MeV W_o = 9.6 MeV

r_r = 1.27 fm r_i = 1.25 fm

a_r = 0.66 fm a_i = 0.47 fm

V_{so} = 7.2 MeV

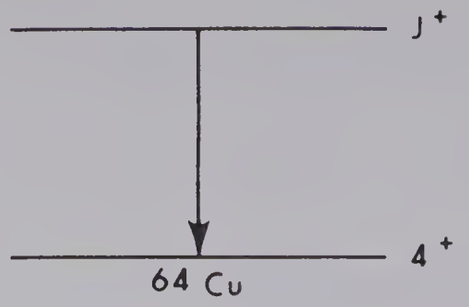

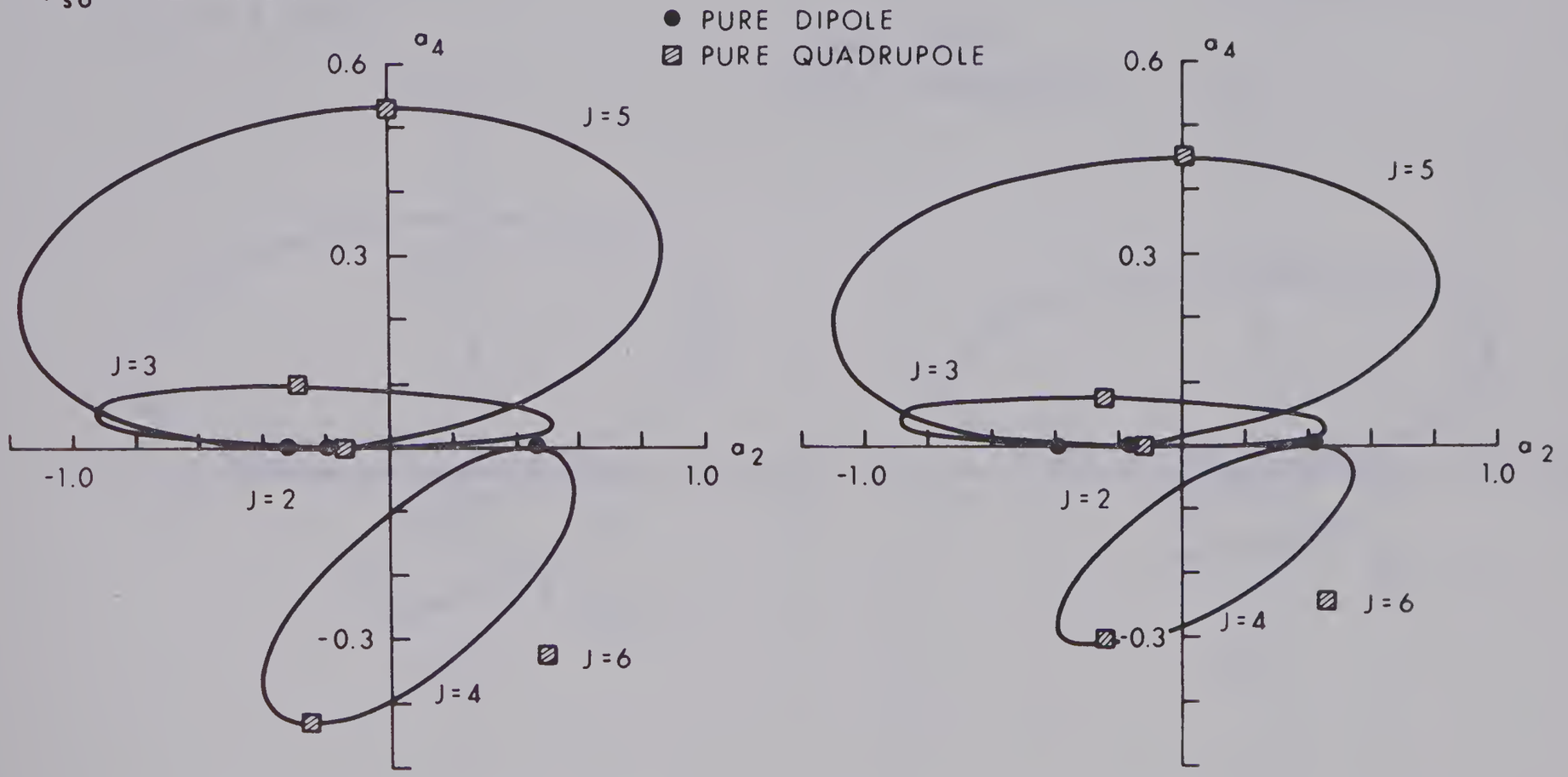

Ep = 50 keV ABOVE THRESHOLD

Ep = 150 keV ABOVE THRESHOLD

Figure 7a

NEUTRON OPTICAL MODEL PARAMETERS

V_o = 48.0 MeV W_o = 9.6 MeV

r_r = 1.27 fm r_i = 1.25 fm

a_r = 0.66 fm a_i = 0.47 fm

V_{so} = 7.2 MeV

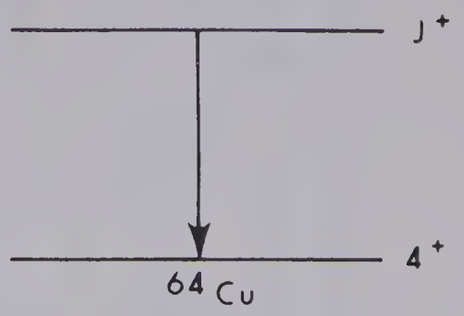

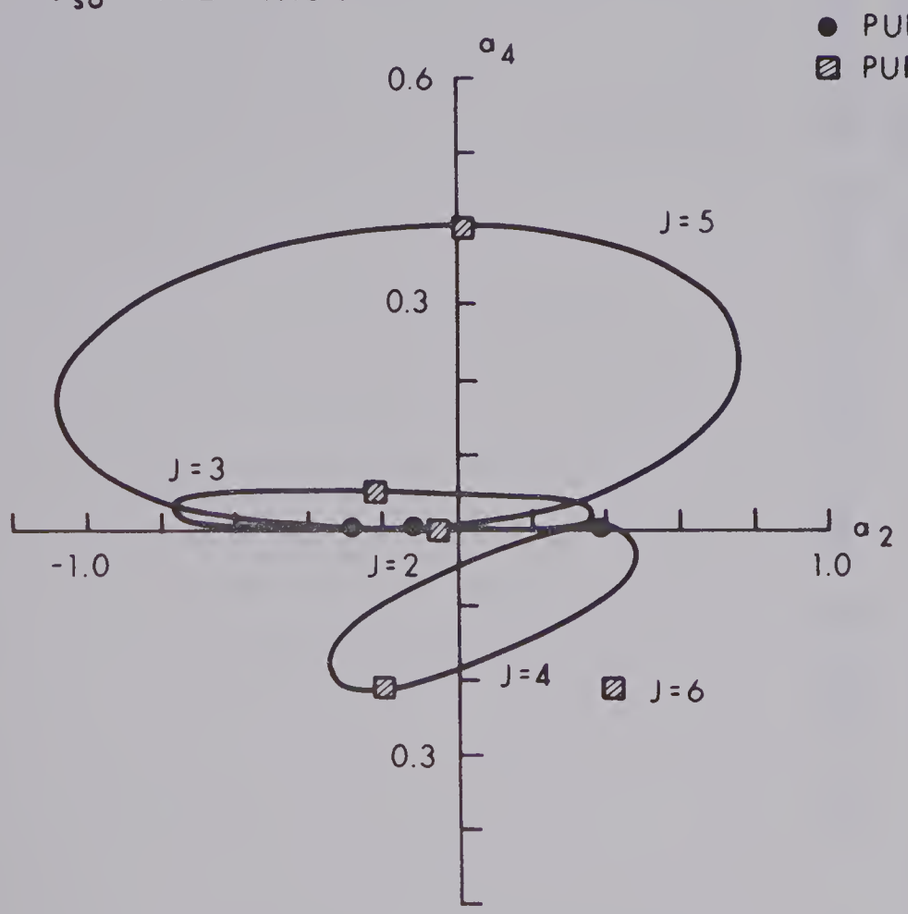

Ep = 300 keV ABOVE THRESHOLD

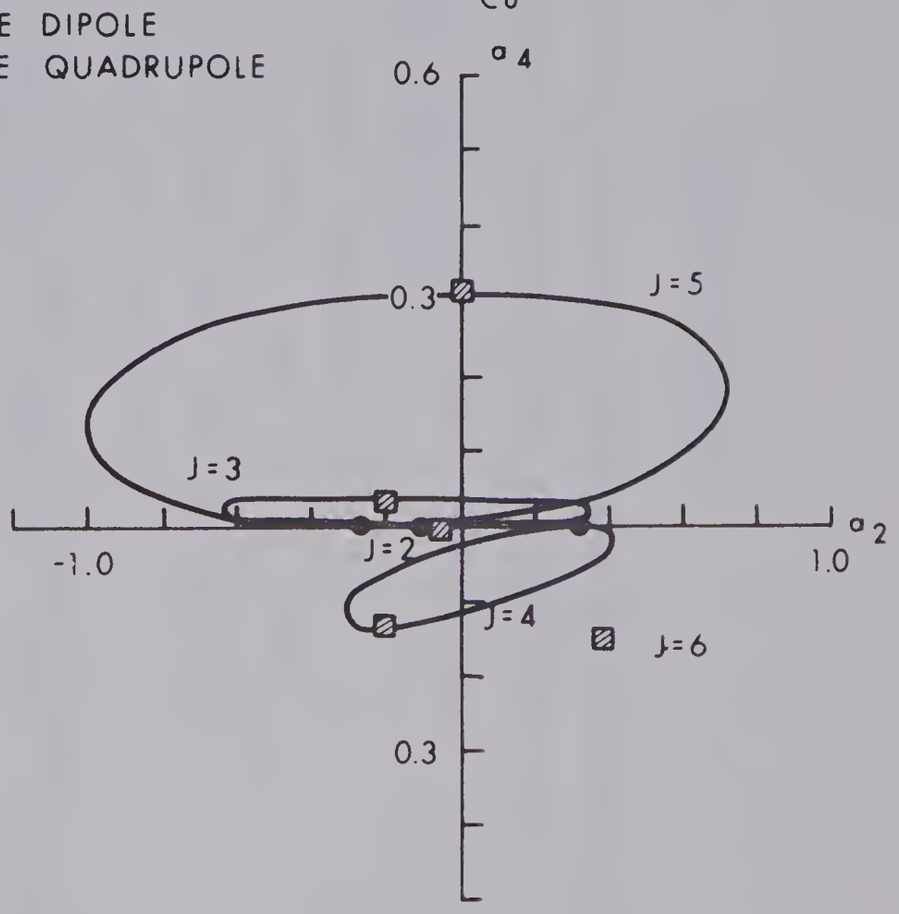

Ep = 500 keV ABOVE THRESHOLD

Figure 7b

APPENDIX REFERENCES

(Bl 52) J.W. Blatt and V.F. Weisskopf, Theoretical Nuclear Physics (1952)

(BF 58) F. Bjorklund and S. Fernbach, Phys. Rev. 109 (1958) 1296

(Da 01) N.E. Davison, University of Alberta, Nuclear Research Center internal report (1969) (unpublished)

(Er 63) T. Ericson, Annals of Physics 23 (1963) 390

(Ha 52) W. Hauser and H. Feshbach, Phys. Rev. 87 (1952) 366

(PB 62) F.G. Perey and B. Buck, Nucl. Phys. 32 (1962) 353

(Pe 63) F.G. Perey, Phys. Rev. 131 (1963) 745

(Ro 66) L. Rosen, Proc. 2^{nd} Int. Symp. on Polarization Phenomena of Nucleons, Karlsruhe, Sept. 1965, ed. P. Huber and H. Schopper, (Birkauser Verlag, Basel (1966) 253)

(Ro 67) H.J. Rose and D.M. Brink, Rev. Mod. Phys. 39 (1967) 306